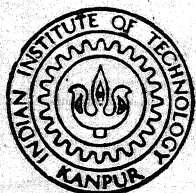


SYNTHESIS AND CHARACTERIZATION OF PURE AND Ca - DOPED Sm—Ba—Cu—O SUPERCONDUCTOR

by

GAUTAM SANKAR BHATTACHARYYA



MATERIALS SCIENCE PROGRAMME
INDIAN INSTITUTE OF TECHNOLOGY KANPUR
DECEMBER, 1989

MSP

1989

M

BHA

SYN

SYNTHESIS AND CHARACTERIZATION OF PURE AND Ca - DOPED Sm—Ba—Cu—O SUPERCONDUCTOR

*A Thesis Submitted
in Partial Fulfilment of the Requirements
for the Degree of*

MASTER OF TECHNOLOGY

by

GAUTAM SANKAR BHATTACHARYYA

to the

**MATERIALS SCIENCE PROGRAMME
INDIAN INSTITUTE OF TECHNOLOGY KANPUR**

DECEMBER, 1989

Dedicated to my

BELOVED PARENTS

- 5 APR 1990

CENTRAL LIBRARY
I. I. T., KANPUR

Acc. No. 107891

Th

620.112972


B469 8

ISP-1989-M-BHA-SYN

CERTIFICATE

This is to certify that Mr. G.S. Bhattacharyya has done work on "SYNTHESIS AND CHARACTERIZATION OF PURE AND Ca-DOPED Sm-Ba-Cu-O SUPERCONDUCTOR" under my supervision and this has not been submitted elsewhere for a degree.

December, 1989.


(K. SHAHI)
Assistant Professor
Materials Science Program
Indian Institute of Technology
Kanpur

ACKNOWLEDGEMENTS

It is my great pleasure to acknowledge Dr. K. Shahi. I think, any thing conveying my gratitude to him is nothing but beggar description. His patience and his constant meticulous guidance has hiked my expectation about guidance in further research field. It is really worthwhile to work under him.

I am conveying my gratitude to Mr. V.P.N. Padmanaban for his constant advice and help. Besides that I am greatly indebted to Mr. Manoravi and Ms. Shiuli Gupta, and Ms. Sujata Chaklanobish and all my lab. mates.

I am fortunate enough to get friends like Mr. Imon Mookerjee and Mr. M.G. Bhangui except their help my work would not be completed.

I am thanking all my ACMS people for their spontaneous cooperations.

I am acknowledging the persons who are indirectly behind my work and my life style to enjoy a pleasant life in IIT Kanpur.

This part would be remain incomplete if I am not conveying my gratitude to Mr. U.S. Mishra for his elegant typing.

-Gautam Sankar Bhattacharyya

CONTENTS

	<u>Page</u>
CHAPTER 1 INTRODUCTION	1
1.1 Introduction	1
1.2 BCS Theory	5
1.3 Review on High T_c Superconductors	10
1.4 Recent Trends in High T_c Superconductors	13
1.5 Some Salient Features of Superconductors	14
1.5.1 D.C. and A.C. Conductivity	14
1.5.2 Heat Capacity	15
1.5.3 Magnetic Property	16
1.5.4 Flux Quantization and Persistent Current	19
1.5.5 Type I and Type II Superconductors and Diamagnetic Behaviour	19
1.6 Application of High T_c Superconductors	21
1.6.1 High Power Magnetics	21
1.6.2 Low Frequency Detection Radio Antennae	21
1.6.3 Superconducting Linear Accelerators	21
1.6.4 Accumulation of Energy	22
1.6.5 Utilization of Josephson Junction	22
1.6.6 Meissner Effect and Its Application	22
1.7 Statement of the Problem	23
CHAPTER 2 EXPERIMENTAL DETAILS	25
2.1 Materials Synthesis	25
2.1.1 Furnace	29
2.1.2 HCHC Die	32
2.2 X-ray Diffraction for Phase Characterization	34
2.3 Measurement of Electrical Resistivity	34
2.3.1 Sample Holder	34
2.3.2 Measurement of Resistivity	33
2.4 Measurement of Thermoelectric Power	38
2.4.1 Sample Holder	38
2.4.2 Measurement of Thermoelectric Power	42

CHAPTER 3	RESULTS AND DISCUSSION	44
3.1	Materials Synthesis	44
3.2	Material Characterization by XRD	45
3.2.1	Pure $\text{SmBa}_2\text{Cu}_3\text{O}_{7-\delta}$ (A_1 , A_2 Samples)	49
3.2.2	Ca-Doped B_1 , B_2 Samples	49
	($\text{SmBa}_{1.5}\text{Ca}_{0.5}\text{Cu}_3\text{O}_{7-\delta}$)	
3.3	Electrical Resistivity Measurement	51
3.3.1	Pure $\text{SmBa}_2\text{Cu}_3\text{O}_{7-\delta}$ (A_1 - A_2 Samples)	51
3.3.2	Ca-Doped $\text{SmBa}_2\text{Cu}_3\text{O}_{7-\delta}$ (B_1 - B_2 Samples),	53
	($\text{SmBa}_{1.5}\text{Ca}_{0.5}\text{Cu}_3\text{O}_{7-\delta}$)	
3.3.3	The Effect of Heat Treatment	56
	($\text{SmBa}_2\text{Cu}_3\text{O}_{7-\delta}$ (A_1 to A_2 Samples)	
3.3.4	The Effect of Doping	59
3.3.5	Combined Effect of Heat Treatment and Doping	
3.4	Thermoelectric Power	60
3.4.1	Thermo Electric Power of Pure	62
	($\text{SmBa}_2\text{Cu}_3\text{O}_{7-\delta}$)	
3.4.2	Thermo Electric Power of Ca-doped	67
	Sm-Ba-Cu-O Samples (B_1 and B_2)	
3.4.3	The Effect of Heat Treatment ²	69
3.4.4	Effect of Doping	72
3.4.5	Combined Effect of Doping and Heat Treatment on Thermo Electric Power	72
3.5	Conclusion	
REFERENCES		76

ABSTRACT

Pure and Ca-doped $\text{SmBa}_2\text{Cu}_3\text{O}_{7-\delta}$ high T_c superconductors have been prepared under two differing conditions. The first route involves heating the reactants at 1173K and sintering twice at 1198K. For the other route these temperatures were 1198K and 1223K respectively. All samples have been characterized by XRD, electrical resistivity (ρ) and thermoelectric power (S) measurements.

New samples holders for four probe resistivity, and thermoelectric power measurements were designed and fabricated locally by us.

All the three studies (XRD, ρ and S) on all the samples suggest that the materials prepared and processed at higher temperatures show better superconducting properties such as lower ρ , higher critical temperature (T_c), lower thermoelectric power (S) and lower width of critical region (ΔT_c). On the other hand Ca-doping in Sm-Ba-Cu-O system does not seem to have favourable effect.

The transport studies ρ and S Vs. T are found consistent with each other. The latter studies indicate that holes are the majority charge carriers, as in $\text{YBa}_2\text{Cu}_3\text{O}_{7-\delta}$ system.

CHAPTER 1

1.1 INTRODUCTION

Low temperature physics or cryogenics as we understand it today was born in 1908 with the successful liquification of helium (below 4.2K) at Leiden by emeritus Dutch physicist H. Kamerlingh Onnes¹. Onnes promptly used liquid helium in a variety of studies of metals at low temperatures and surprisingly observed in 1911 that the electrical resistance of pure mercury dropped abruptly to zero upon cooling to below 4.2K (Fig. 1.1). To Onnes surprise, the addition of impurities to the mercury failed to provide any residual resistance at the lowest temperature and by 1913 he concluded that "Mercury has passed into a new state, which on account of its remarkable electrical properties may be called the superconductive state". Material is superconducting below or at a particular temperature called superconducting transition temperature or critical temperature denoted by T_c .

Superconductivity is a nice depiction of macroscopic quantum state of materials. But for many years it remained as a matter of laboratory curiosity. The reasons were two fold.

- (a) It was an academic study with no apparent prospect of applications, and
- (b) For almost half a century the phenomenon defied explanation.

However, due to persistent efforts of the scientists, the subject has undergone a dramatic change.

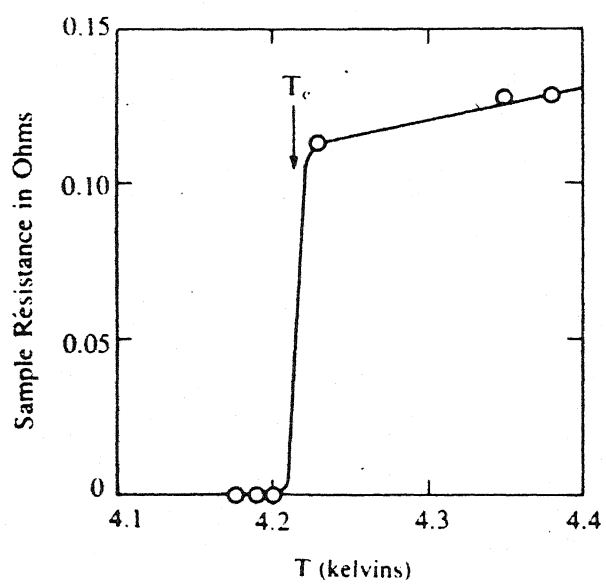


Figure: 1.1

It was recognised quite early that the superconducting state represented a distinct thermodynamic phase. This made some aspects of superconductivity less mysterious but raised new and more difficult questions. One of them was smallness of the condensation energy. Although it seemed that condensation was purely electronic in nature, but why was the condensation energy not comparable in magnitude with the Fermi energy.

An even more fundamental problem was the nature of interaction responsible for superconductivity.

Froehlich² in the year 1950 observed that Bloch's³ theory of metallic conduction could be formulated as a field theory. As per field theory the mechanism responsible for electrical resistance is scattering of electrons with associated emission or absorption of quanta (phonons) of the acoustic vibration field of the medium. This electron-phonon interaction suggests an attractive electron-electron interaction. According to Froehlich, this was the interaction responsible for superconductivity. This immediately received striking experimental confirmation with the discovery of the isotope effect. But early attempts to construct a perturbation theoretical model based on Froehlich's interaction encountered severe mathematical difficulties. It gradually became clear in the words of Casimir⁴, "it may be just as difficult to find the actual superconducting state by perturbation method,

as it would be, to find the crystal structure of solid argon starting from the ideal gas law. In this latter case we can obtain a good approximation to the thermodynamic function of both solid and gas if we start from the right model. In a similar way I believe that one should try to make a good guess as to what the state of affairs is and thus calculate the energy."

In 1951 Onsager⁵ conjectured that conduction electrons might form "quasi-molecular" pairs bound by the Froehlich interaction. These pairs would have Boson properties and might undergo a Bose-Einstein condensation. Such conjectures were motivated by the widely accepted belief e.g. Ginzburg⁶ that a condensed Bose gas of charged but non-interacting particles would have superconducting properties. In 1955 Schafroth⁷ rigorously demonstrated this property of the charged Bose gas. Much effort was spent on the search for a Bose-gas model, see for example Schafroth et.al.⁸. But the "Good Guess" hoped for by Casimir actually came in a form somewhat different from Onsager's conjecture. Although the electrons are paired and the pairs now overlap considerably and the condensate is not a simple Bose condensate.

Ultimately in 1956 Cooper⁹ showed that the Fermi sea is unstable against pair formation when there exists any attractive interaction, however small between electrons.

In the light of Cooper's result, Bardeen, Cooper and Schrieffer¹⁰ in the year 1957, constructed a variational wave function for a ground state with complete electron pairing and orthogonal functions for low-lying excited states having only a few such pairs broken. This theory is abbreviated as "BCS Theory".

1.2 BCS THEORY

Bardeen, Cooper and Schrieffer¹⁰ proposed a theory for superconductors to specify an interaction mechanism between the electrons. In many superconductors, the following relationship between T_c and the atomic mass (M) is observed.

$$T_c = M^{-0.5}$$

which indicates that the vibrational motion of the heavy nuclei must play an essential role.

In both normal and superconducting states a Coulomb repulsion between pairs of electrons exists which is screened by the presence of other electrons. The electrons in a solid interact with the lattice vibrations by emitting or absorbing phonons, and the effective interaction between the electrons can arise from the exchange of phonons which is attractive by nature.

The phonons may be "virtual" as by uncertainty principle, energy conservation is not required in the

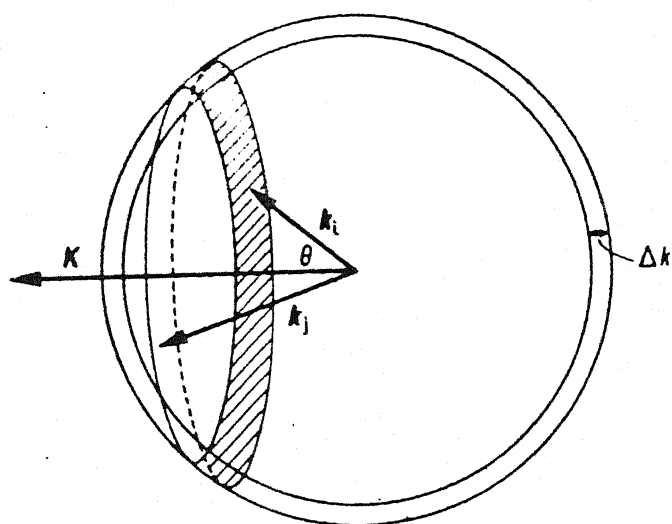


Figure: 1.2

transitional state if an emitted phonon is reabsorbed by a second electron in a very short time. Phonon existence is the movement of ions and attraction can be predicted by imaging one electron of the pair surrounded by a distribution of positive charges due to the ion movement. As per BCS theory, attraction due to phonon exchange should exceed the screened Coulomb repulsion. So in superconductors, pairs with zero total momentum are the most likely.

Consider two electrons in states \vec{k}_i and \vec{k}_j with energies equal to the Fermi energy (Fig. 1.2) so that

$$\vec{k}_i = \vec{k}_j = \vec{k}_F \quad (1)$$

Total momentum of the pair is

$$\vec{K} = \vec{k}_i + \vec{k}_j \quad (2)$$

For a definite value of \vec{K} where,

$$\vec{K} = 2\vec{k}_F \sin\theta \quad (3)$$

Only the electron states on the ring can form such pairs. But for $\vec{K} = 0$, $\vec{k}_i = -\vec{k}_j$, all the electron states on the Fermi sphere can be paired. Thus pair states with $\vec{K} = 0$ are much more likely to occur than states with finite \vec{K} . Strictly because of the finite phonon energy $\hbar\omega(q)$, only electron states in a shell of width Δk , where

$$\hbar^2 k_F \Delta k / m = \hbar \omega (q) \tag{4}$$

can take part so that a finite shell of \vec{k} states is involved but this does not invalidate the conclusion. The pairs also hold the sanctity of Pauli's Exclusion Principle. In superconductors at $k = 0$. All the electrons in states near the Fermi surface are bound into pairs (ground state configuration). The finite energy 2ϵ is required to break pairing and to produce single normal electron. So no energy exists between the ground state and 2ϵ , so energy gap exists and is given by,

$$2\hbar\omega_L \exp [-1/S(E_F)G] \tag{5}$$

where

- $\hbar\omega_L$ - Average phonon energy accounts for isotope effect
- $S(E_F)$ - Density of electron states at Fermi energy
- G - Measure of strength of the electron-phonon-interaction.

So higher the value of G more the chances of superconductivity.

Since ground state is a pairing state there is no chance of scattering of electrons unless electrons gain sufficient energy to cross the gap. Hence for $T < T_c$ there is no resistance to current. If the electrons at the Fermi surface drift with velocity v , they gain an extra energy (E)

expressed by

$$E = (\hbar k + m v)^2 / 2m - \hbar^2 k^2 / 2m \approx \hbar k v \quad (6)$$

When this energy is greater than the gap, i.e., when v exceeds a critical velocity v_c then

$$v_c \approx \epsilon / \hbar k_F \quad (7)$$

the superconductivity will disappear due to beginning of scattering. To break this pairing, thermal energy and optical excitations are sufficient.

The coherence length ξ_0 can be related to energy with the help of the uncertainty principle. The range in electron Δp , associated with the energy gap is given by

$$\Delta p \hbar k_F / m \approx \epsilon \quad (8)$$

The coherence length is given by,

$$\xi_0 = \hbar / \Delta p \approx \hbar^2 k_F / m \epsilon \approx 10^{-4} \text{ cm} \quad (9)$$

The difference between the energy in the normal and the superconducting states arises due to formation of gap. And a number $GS(E_F)$ of electrons have changed their energy by an amount 2ϵ . So for Type I superconductors we have

$$B_c^2/2\mu_0 = 0.5 S(E_F)\epsilon^2 \quad (10)$$

where,

B_c - critical magnetic field.

But density of states is related to the normal electronic specific heat $\gamma.T$ and can be expressed by

$$B_c^2/\mu_0 T_c^2 \approx 0.5 \gamma \quad (11)$$

Thus, according to BCS theory, maximum critical temperature of superconductors cannot exceed (30-40)K.

1.3 REVIEW ON HIGH T_c SUPERCONDUCTORS

Onnes discovery of superconductivity was not secluded but rather it was tried to perambulate to the betterment i.e. to achieve higher T_c . Metals were tested without profound effect, so alloys were the next natural choice. In the year 1973, the target was germanium niobate and ($T_c \approx 23.3$ K), though the rise of T_c was remarkable but still the goal of higher T_c to help the society seemed to be impossible. But scientists were then also trying to pierce the realms of higher T_c .

As a result in the year 1986 Bednorz of "IBM Zurich" while working with La-Ba-Cu-O system, found that T_c could be

improved to 30K with alteration of barium concentration.

Bednorz and Muller's investigation on some mixed compounds in the year 1983 was a significant step forward towards high T_c superconductivity. Meanwhile Michel et.al.¹¹ published a paper on copper oxide with variable valency state. So Bednorz and Muller¹² stepped into the copper oxide system. They selected lanthanum barium copper oxide system as a matter of interest. In this system, barium (Ba^{2+}) is divalent, lanthanum (La^{3+}) is trivalent and oxygen (O^{2-}) is always divalent. So it is copper which should be in mixed valence state to make the system electrically neutral. It is found copper is in Cu^{+2} or Cu^{+2} state simultaneously with different proportions as per requirements. It is also found that the amount of mixed valency is controlled by the concentration of barium ions in the system.

By January 1986, Bednorz and Muller¹² had synthesized a 90K superconductor. Their sample was prepared by coprecipitation method. They found that the resistivity varied almost linearly with temperature, like those of normal metals, between room temperature and T_c , and suddenly dropped to zero at the critical temperature T_c . This was a sure sign of superconducting behaviour which shocked many who believed that ceramics were necessarily insulators. This piece of work by Bednorz and Muller¹² has since 1986 opened a new era of research and development on high T_c superconductors.

The phase characterization studies on these La-Ba-Cu-O of the samples revealed that it is a multiphasic compound with three phases. The first one is copper oxide (CuO) which is naturally an insulator (ceramic compound) the second one is $\text{Ba}_x\text{La}_{5-x}\text{Cu}_5\text{O}_{5(3-y)}$ - a metallic compound. The third phase is $\text{Ba}_x\text{La}_{2-x}\text{CuO}_{4-y}$. It contained a small proportion of barium.

BaO has the well known K_2NiF_4 type layered structures. The CuO_6 is octahedral but Ba and CuO_6 forms a Perovskite structure. Actually oxygen defects alternate with layers of LaO. This LaO phase is superconducting.

At Houston Chu¹³ and his coworkers while working on the effect of high pressure on Barium compounds found some positive results. At the University of Alabama Huntsville. Chu¹³ group joined Wu¹⁴ group and replaced Lanthanum by yttrium and found a T_c of 92K in a multiphase yttrium-barium-copper-oxide system.

Maeda¹⁵ and his group at National Research Institute for Metals (NRIM) has recently reported as high a T_c as 120K for Bi-Ca-Sr-Cu-O system which is also multiphase. A T_c of \sim 120K was also found in Tl-Ca-Ba-Cu-O system by Shen and Hemen¹⁶ recently.

At present the wave of research on the high T_c superconductivity is drenching each and every low temperature laboratory of the world. A very large number of scientists and technologists are currently engaged in developing new high T_c materials and exploring their applications in various

devices. The recent thrust clearly is directed at synthesizing superconductors with higher T_c , preferably near room temperature. And, if the developments of the last few years are any indication, the possibility of a room temperature superconductor in near future cannot be ruled out.

1.4 RECENT TRENDS IN HIGH T_c SUPERCONDUCTORS

Bednorz and Müller¹² have reported that $\text{La}_{5-x}\text{Ba}_x\text{Cu}_5\text{O}_{5(3-y)}$ system, (where $x \leq 1$) on cooling the resistivity of the sample with the value of x first goes down and then goes up just before the abrupt drop commencing at 35K. Some samples have zero resistivity below 12K though all are multiphasic.

Wu et.al.¹⁴ reported superconductivity at 92K in Y-Ba-Cu-O system at ambient pressure. Cava et.al.¹⁷ prepared a single phase Y-Ba-Cu-O system which has a distorted orthorhombic oxygen deficient perovskite structure of stoichiometry $\text{YBa}_2\text{Cu}_3\text{O}_{9-\delta}$ ($\delta \leq 2.1$) with unit cell constants $a = 3.822 \text{ \AA}$, $b = 3.891 \text{ \AA}$ and $c = 11.677 \text{ \AA}$ and a $T_c = 91\text{K}$. The modern trend now is to replace one, two or even three elements of Y-Ba-Cu-O system to achieve higher T_c . The results on several dozen substituted Y-Ba-Cu-O systems are available. However, it appears that the substitution is unable to alter the T_c significantly. Nevertheless the effort should be worthwhile.

Maeda and coworkers¹⁶ have reported a T_c of 120K for Bi-Ca-Sr-Cu-O system which is multiphase and resistivity measurements show a two step transition at 110K and 75K in

Bi-Ca-Sr-Cu-O system. The lower T_c transition was indifferent to the composition, while higher T_c was not observed after prolong annealing below 1073K. Shen et.al.¹⁶ recently reported T_c 120K for Tl-Ca-Ba-Cu-O system.

Now we have to wait to see that who will break the ice next to get higher T_c or even T_c at room temperature? Only time is the best teller of the fact. We hope that the ravenous thirst lips of the scientists one day will feel a sweet sip.

1.5 SOME SALIENT FEATURES OF SUPERCONDUCTORS

1.5.1 D.C. AND A.C. CONDUCTIVITY

D.C. conductivity of a superconductor is infinite, and therefore, any current initiated in a closed loop of a superconducting material should persist for a very very long time without any need for a driving electromotive force.

But if a superconducting loop has an inductance L and a finite resistance R , then persisting current should slowly decline according to the following relationship:

$$I = I_0 \exp (-Rt/L) \quad (1)$$

where,

I_0 = initial current,

t = time elapsed.

According to Bardeen, superconducting state is better to define as a perfect diamagnetic state than a state of infinite conductivity. Since at $T = 0$ K the conductivity is infinite

only upto a limiting frequency and at a finite temperature ($<T_0$) there is a small A.C. loss at all frequencies.

1.5.2 HEAT CAPACITY

There is no heat of transformation associated with superconducting to normal transition in a metal. But there is an anomaly in the electronic component of the specific heat. The discontinuity in the specific heat shows the second order transition from a relatively disordered (normal) state to a more highly ordered (superconducting) state of lower entropy. A similar specific heat anomaly occurs when liquid helium becomes superfluid and it is quite useful to regard a superconducting metal as a superfluid medium (the Bosons involved being electron pairs with opposite spin and momentum as per BCS theory).

The electron waves in superconducting state are coherent over microscopic distances. For a metal in normal state the sum of the total specific heat is the contribution due to T^3 term, i.e. lattice vibrations (Debye Law term) and are directly to the absolute temperature representing the temperature dependence of energy for a Fermi electron gas.

The contribution of the phonons is unchanged in the superconducting state, but the electronic term is much more strongly temperature dependent. In some superconducting metals

only upto a limiting frequency and at a finite temperature ($<T_0$) there is a small A.C. loss at all frequencies.

1.5.2 HEAT CAPACITY

There is no heat of transformation associated with superconducting to normal transition in a metal. But there is an anomaly in the electronic component of the specific heat. The discontinuity in the specific heat shows the second order transition from a relatively disordered (normal) state to a more highly ordered (superconducting) state of lower entropy. A similar specific heat anomaly occurs when liquid helium becomes superfluid and it is quite useful to regard a superconducting metal as a superfluid medium (the Bosons involved being electron pairs with opposite spin and momentum as per BCS theory).

The electron waves in superconducting state are coherent over microscopic distances. For a metal in normal state the sum of the total specific heat is the contribution due to T^3 term, i.e. lattice vibrations (Debye Law term) and are directly to the absolute temperature representing the temperature dependence of energy for a Fermi electron gas.

The contribution of the phonons is unchanged in the superconducting state, but the electronic term is much more strongly temperature dependent. In some superconducting metals

specific heat due to electrons varies roughly with T^3 at low temperature and given by

$$C_p = AT^3 + B \exp(\sigma \cdot T^{-1})$$

where A, B, and σ are constants. The energy gap between normal state and superconducting state is of the order of $4 \cdot K_0 \cdot T_c$, i.e., electrons can be thermally excited to normal state. So at absolute zero entropy and specific heat both are zero.

1.5.3 MAGNETIC PROPERTY

It is well known that the superconductivity survives only if the external magnetic field is less than a critical field (H_{c1}). This quantity varies from a maximum value H_0 at 0 K to zero field at T_c . For many super conductors the temperature dependence is as follows:

$$H = H_0 [1 - (T/T_c)^2]$$

This is often called Tyn's law.

Meissner and Ochsenfeld¹⁸ showed that the superconducting state is independent of any previous magnetic environment and a metal cooled through the superconducting transition temperature expels all flux lines from its interior (if

field = H_c , no flux is expelled as material is no longer superconducting). Any flux lines expelled from inside must be offset by an induced persistent surface current. Termination of the external field induces an opposite surface current which in turn cancels the former one and leaves the superconductor both field free and current free. This Meissner effect of flux expulsion makes the transition between the superconducting and normal states reversible. Unlike the electric field, magnetic field can penetrate a superconductor to a depth of λ (10^{-8} to 10^{-7})m.

$$\lambda = [m \epsilon_0 c^2 / e^2 n_s]^{0.5}$$

where

- λ = Penetration depth
- n_s = Superconducting electron density
- c = Velocity of light
- ϵ_0 = Permittivity
- e = Electronic charge
- m = Mass of electron.

As temperature approaches T_c the number of superconducting electrons tend to become zero which implies infinite penetration, i.e., $\lambda \rightarrow \infty$. The penetration of field varies with temperature as follows:

$$\lambda = \lambda_0 [1 - (T/T_c)^4]^{-0.5}$$

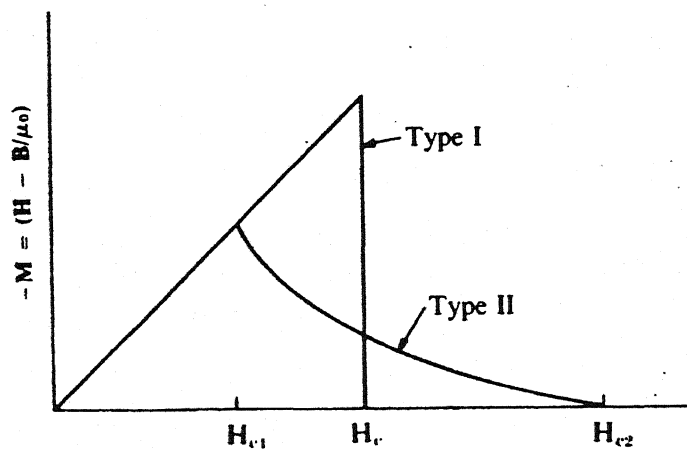


Figure: 1.3

1.5.4 FLUX QUANTIZATION AND PERSISTENT CURRENT

If we take a hollow cylinder and the body is also a superconductor then the flux in the material is expelled but surprisingly the flux in the hole is not expelled but rather trapped inside and having infinite conductivity of the hollow cylinder. If we remove the external field the cylinder will carry required amount of current to preserve the flux through the cylinder. This is called persistent current. The flux is quantized and given by,

$$2\pi\hbar/e = 4.14 \cdot 10^{-15} \text{ wb}$$

The persistent current decays in a quantized manner.

1.5.5 TYPE I AND TYPE II SUPERCONDUCTORS AND DIAMAGNETIC BEHAVIOUR

There are two types of superconductors, one is Type I and another is Type II. Type I includes elements like Cd, Zn, Pb, etc. which are satisfactorily described by the BCS theory. Type II superconductors are compounds formed from transition and actinide series elements, and include most of the superconducting compounds.

If a Type I superconductor is fabricated as a long solid cylinder with zero demagnetizing factor, then in the

presence of an applied field ($< H_c$) the sample sets up circulating surface current, which makes $B = 0$, in the interior. The variation of magnetization with the field is shown in Fig.1.3 for Type I superconductors. Above the critical field H_c , the conduction of the metal has been forced to become normal and B/μ_0 inside the solid would differ from H outside the solid, only to the some small degree as in any other paramagnetic solid. For Type I superconductors the wave functions are coherent over distances much larger than the penetration depth and it takes less energy to create a single external barrier between the magnetic field and the superconductor than it does to permit a filamentary structure.

For Type II superconductors the behaviour is different in a magnetic field (Fig. 1.3). This type of material permits some penetration of magnetic flux above a first critical field H_{c1} . For fields greater than H_{c1} but less than H_{c2} the material is said to be in an intermediate state. For a hard type II superconductor H_{c2} is very large ($\leq 10^7$ A/m. T = 0 K]. A type II superconductor has infinite DC conductivity in the intermediate state though it consists of a mozaic of filaments of normal and superconducting materials. For Type II superconductors the coherence length associated with superconducting state wave function is smaller than the Landau penetration depth

1.6 APPLICATION OF HIGH T_c SUPERCONDUCTORS

1.6.1 HIGH POWER MAGNETS

The most widespread use of all superconducting devices to date is the superconducting magnet, which uses a large direct current in a coil of superconducting wire to generate a high magnetic field for laboratory or industrial use. Though the disadvantage is that it needs liquid nitrogen, yet the zero I^2R loss more than compensates the cost of using liquid nitrogen. And a large current can be passed to get a high magnetic field. The type II superconducting materials have high H_{c2} value at operating conditions. But manufacturing problem is the brittleness of the material.

1.6.2 LOW FREQUENCY DETECTION RADIO ANTENNAE

The detection of low frequency signal is very difficult as the antennae have well enough electrical resistance. But the antennae made from superconducting material undoubtedly offers the best solution to the problem of weak-signal reception whether from deep sea or from polar region or from the outer space.

1.6.3 SUPERCONDUCTING LINEAR ACCELERATORS

In superconducting linear accelerators, the microwave resonant cavities are lined with a thin layer of lead or niobium, cooled with supercooled helium. A superconducting LINAC at Stanford University operates at 950 MHz frequency

and can achieve a Q value of the order of 10^{10} within the resonant cavities.

1.6.4 ACCUMULATION OF ENERGY

In superconductors resistivity is zero, so also is I^2R loss for all practical purposes and hence once current introduced is not decayed so energy can be stored within the superconductors.

1.6.5 UTILIZATION OF JOSEPHSON JUNCTION

"SQUID" i.e. superconducting quantum interference devices are used in very high speed logic switches in analog to digital converters. SQUIDS are efficient in detecting very little change in magnetic field hence their main applications are in prospecting for minerals and oils and imaging atomic structures etc. They can also be used to measure magnetic pulses generated by human brain and hearts. With the help of Josephson junction computer technology as far as speed is concerned can be tremendously increased.

1.6.6 MEISSNER EFFECT AND ITS APPLICATION

Superconductor is a perfect diamagnet, so levitation can be made possible. This principle can be used for running trains on magnetic tracks. This will curtail the fuel cost due to aversion of friction which is present in the conventional railway tracks and the speed of the train can also be tremendously increased.

1.7 STATEMENT OF THE PROBLEM

Ever since the discovery of superconductivity in ceramic oxides by Bednorz and Muller in 1983, an unprecedented effort has been layered by the scientists all over the world to develop superconductors with T_c near or at room temperature. $YBa_2Cu_3O_{7-\delta}$ system is one of the most widely studied high temperature superconductors which has a $T_c \sim 90K$. In this system number of dopants for Y , Ba and Cu and variations in preparational conditions (reaction and sintering temperatures, atmosphere etc.) have been tried in order to achieve higher T_c . However the synthesis of this material often leads to a mixture of at least two phases, tetragonal and orthorhombic $YBa_2Cu_3O_{7-\delta}$ and thereby makes the interpretation of the results much more difficult.

The aim of the present work was to investigate the effect of variations in preparational parameters such as reaction temperature (T_R), sintering temperature (T_S), duration of reaction and sintering processes and the effect of dopants on the superconducting properties such as T_c , resistivity, thermoelectric power, etc. $Sm-Ba-Cu-O$ system was chosen as the base material primarily because it is easily synthesised in single phase as is a relatively new material. The samples of $Sm-Ba-Cu-O$ were reacted at two different temperatures (1173K or 1198K) and also sintered at two different temperatures, 1198K and 1223K respectively. Both samples were soaked at 883K.

In addition to this sample, Ca-doped samples, viz. Sm-Ba-Ca-CuO were also prepared following the above procedures. All the samples have been characterized by XRD, electrical resistivity and thermoelectric power measurements.

CHAPTER 2

2.0 EXPERIMENTAL DETAILS

Our main interest was to study the effect of Ca-doping and variation in the preparational conditions such as reaction and sintering temperatures etc on the superconducting properties of $\text{SmBa}_2\text{Cu}_3\text{O}_{7-\delta}$ system. In the following paragraphs, the various steps involved in the materials synthesis as well as the details of materials characterization by X-ray diffraction, electrical resistivity and thermoelectric power measurements are described briefly in the sequence given below.

1. Materials Synthesis
2. X-ray diffraction for phase characterization.
3. Measurement of electrical resistivity
4. Measurement of thermoelectric power

2.1 MATERIALS SYNTHESIS

The purity and other details of the starting materials are given in the Table 1.

TABLE 1

PURITY AND OTHER PROPERTIES OF STARTING MATERIALS

Sm₂O₃ (Samarium oxide)

Manufacturer: Indian Rare Earths Ltd.

Purity : 99.99%

Molecular wt.: 348.70

Crystalline : White yellowish powder
form

Specific : 8.347
gravity

Melting point: -

BaCO₃ (Barium Carbonate)

Manufacturer: Qualigen Fine Chemicals (India)

Purity : 99.8%

Molecular wt.: 197.35

Crystalline : White, hexagonal
form

Specific : 4.43
gravity

Melting point: 2013K

CaCO₃ (Calcium Carbonate)

Manufacturer: Qualigen Fine Chemicals (India)

Purity : 98%

Molecular wt: 100.09

Crystalline : Rhombohedral
form

Specific : 2.930
gravity

Melting point: Transition point to calcite 793K

Continued.....

TABLE 1 (Continued):

CuO (Copper Oxide)

Manufacturer : Alpha Chemicals (USA)
Purity : 99.99%, Ultrapure
Molecular : 79.54
wt.
Crystalline : Black powder, monoclinic
form
Specific : (6.30 - 6.49)
gravity
Melting point : 1599K

Appropriate amounts of Sm_2O_3 , BaCO_3 , CaCO_3 and CuO were weighed using a digital single pan balance (Mettler AE 160) and mixed in mortar and pestle for (2-3) hrs to ensure homogeneity. The mixture was compressed at $\sim 3 \text{ ton cm}^{-2}$ in a steel die to obtain pellets. Low compaction pressure deliberately used to make loose pellet so as to permit exchange of gaseous oxygen between the sample and the environment during reaction. These pellets were subsequently put in a platinum boat, which in turn was kept inside a metre-long quartz tube. The two ends of the quartz tube were sealed with silicon rubber bungs each having a central hole fitted with Teflon tube to permit the flow of oxygen gas.

The assembly was kept in a horizontal electrically heated furnace whose temperature was controlled within $\pm 2\text{K}$. A chromel-alumel thermo couple positioned close to the sample was used to monitor the reaction temperature. A heating rate of (100-150) K/hr was normally employed. The flow rate of oxygen gas was maintained by observing the number of bubbles per unit time through the water bath in the flask, usually a flow of (15-20) bubbles per minute was maintained.

In order to determine the optimum reaction temperature (T_R) samples P and Q were prepared at two different temperatures. T_R is 1173K and 1198K respectively and duration of reaction was (12-16) hrs. After this the pellets were

cooled to room temperature and reground thoroughly and the resulting powder used, to make pellets at a pressure of $\sim 5 \text{ ton cm}^{-2}$. These pellets were sintered at T_s of 1198K or 1223K respectively for ~ 20 hrs followed by cooling to room temperature slowly under continuous flow of oxygen gas. These samples were again heated to 1198K or 1223K respectively and kept for ~ 20 hrs followed by cooling to 833K and holding for ~ 10 hrs i.e. soaking (T_{sk}) and then cooled to room temperature slowly. These samples were used for further studies.

2.1.1 FURNACE

The furnace used for materials synthesis was made in our local workshop which had the provision for the gas flow. The entire assembly shown in (Fig.2.1) consists of the following components:

- i) Furnace
- ii) Temperature controller
- iii) Quartz tube
- iv) Platinum boat
- v) Gas cylinder and regulator.

Kanthal wire (dia 2 mm) wound uniformly (10 turns per inch) over a mullite tube (dia ~ 4.8 cm, length ~ 45 cm) served as

TABLE 2

DETAILS OF HEAT TREATMENT SCHEDULE

Sample 'P'

	Temperature (K)	Time to reach (hrs)	Holding time (hrs)
Reaction temperature (T_R)	1173	6	(12-16)
Sintering temperature (T_s)	1198	6&1/2	20
Sintering temperature (T_s)	1198	6&1/2	20
Soaking temperature (T_{sk})	833	3	10

Sample 'Q'

Reaction temperature (T_R)	1198	6&1/2	(12-16)
Sintering temperature (T_s)	1223	7	20
Sintering temperature (T_s)	1223	7	20
Soaking temperature (T_{sk})	833	4	10

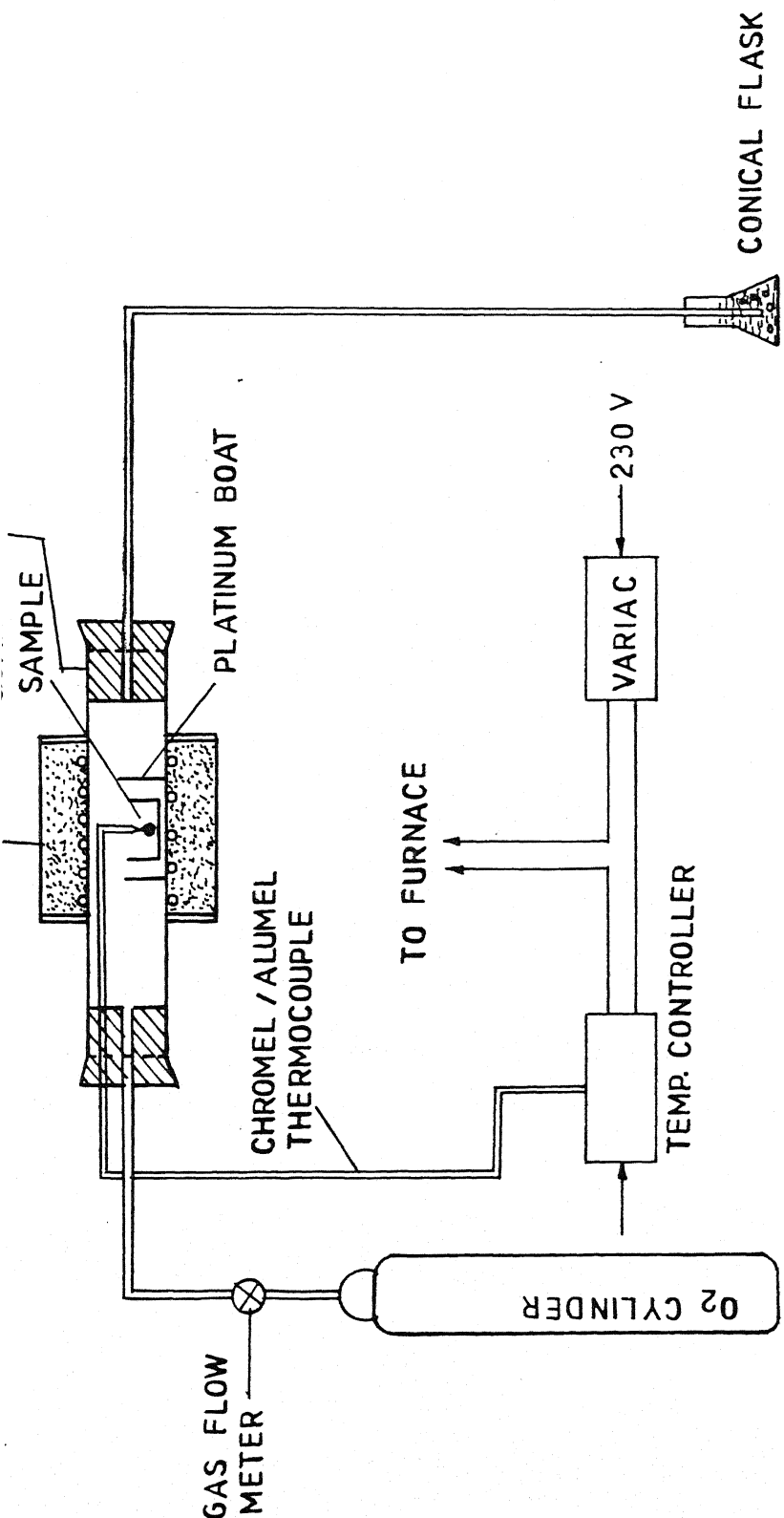


FIG. 2.1 ARRANGEMENT FOR PREPARATION OF HTSC MATERIALS UNDER FLOW OF OXYGEN

the heating element. The total resistance of the heating element was ~ 40 Ohms.

This assembly was housed centrally in a cylindrical aluminium body (Fig. 2.1) and the holder space between the mullite tube and aluminium case was filled with MgO and asbestos powder to minimise the heat loss.

Inside the mullite tube was placed a sufficiently long quartz tube whose ends were sealed with silicone rubber bungs fitted with Teflon tubes (outer dia 7 mm, inner dia 5 mm). The Teflon tube on one side was connected to the gas cylinder while that on the other side to a bubbler. The flow rate of the oxygen gas could be controlled by monitoring the number of bubbles per unit time flowing through the bubbler. Chromel-alumel thermocouple inserted in the quartz tube through the silicone rubber bung was used to sense the temperature.

2.1.2 HCHC DIE

The die was made up of high carbon high chromium steel and consisted of three pieces as shown in (Fig. 2.2). The central cylindrical piece has a through hole of (dia ~ 9 mm), and the two T-shaped plungers of matching diameter to fit in from the top and bottom of the central piece. The highest dia of top plunger is 15 mm and lowest dia is 9 mm. The length of plunger is 59 mm. The highest dia of the bottom plunger is 15 mm and the lowest dia is 9 mm and height of the plunger is 29 mm. The schematic diagram of the die is

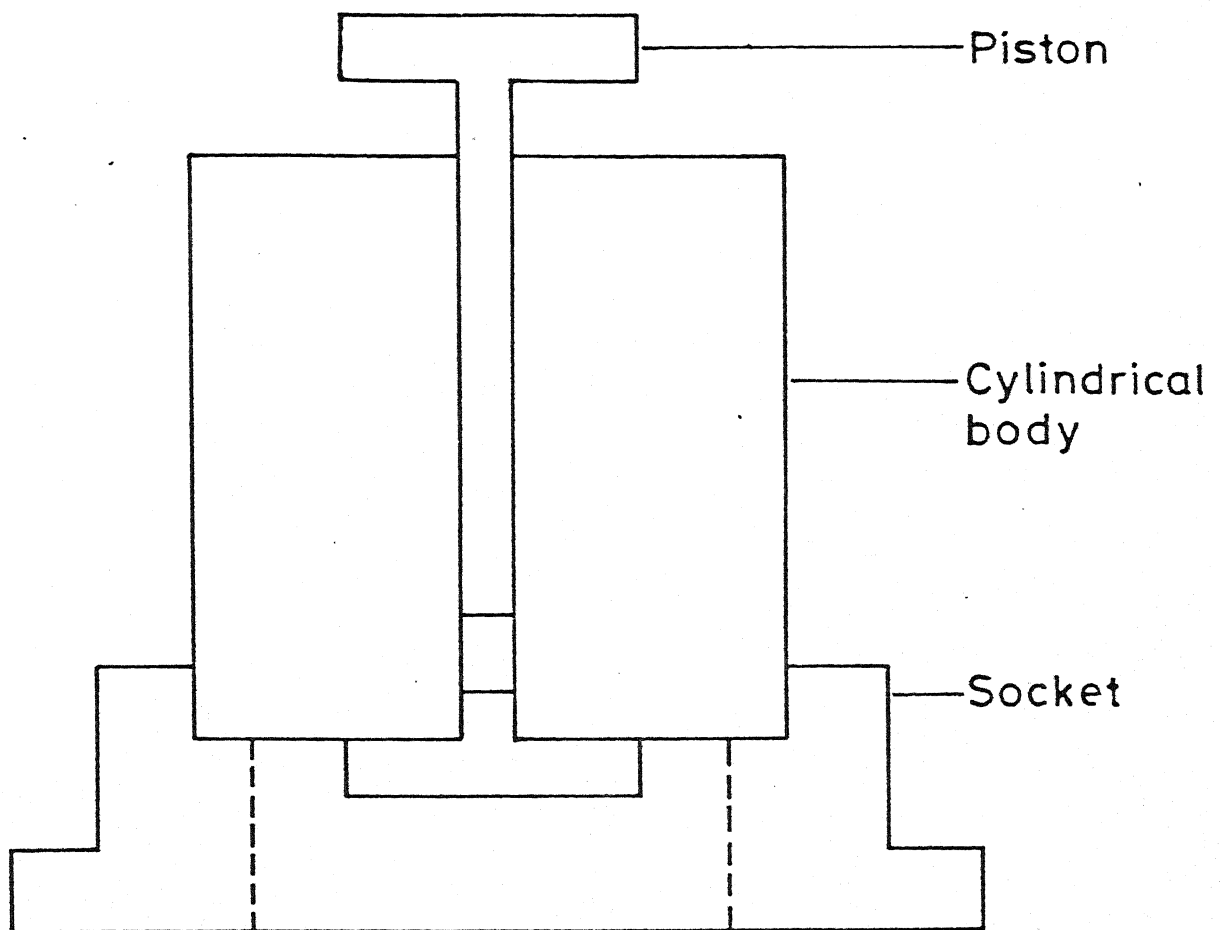


Fig.2.2 Schematic diagram of steel die .

shown in the (Fig. 2.2). The die is then heat treated and oil quenched to harden the material. The next step is grinding of the die. Thus die is made and suitable for using. The die during use is placed on a steel die base, shown in the (Fig. 2.2). During use every element of the die is kept vertical to avoid differential stress and to get uniformly dense pellet.

2.2 X-RAY DIFFRACTION FOR PHASE CHARACTERIZATION

X-ray diffraction (XRD) patterns of various samples were recorded using "Reich Scifert Iso-Debye-fley 2002 Diffractometer". The radiation used is CuK_α ($\lambda = 1.54 \text{ \AA}$). The pellets are put into a rectangular perspex sample holder by using plasticine. The surface is levelled by pressing it with a glass plate over it.

The XRD patterns are recorded in the 2θ range of 20° to 70° .

The XRD is done just to see the peaks at different angles. It is seen that the orthorhombic peak is coming at the angle of 32.54° in terms of 2θ value. The various XRD patterns are shown in the (Fig. 3.1- 3.4).

2.3 MEASUREMENT OF ELECTRICAL RESISTIVITY

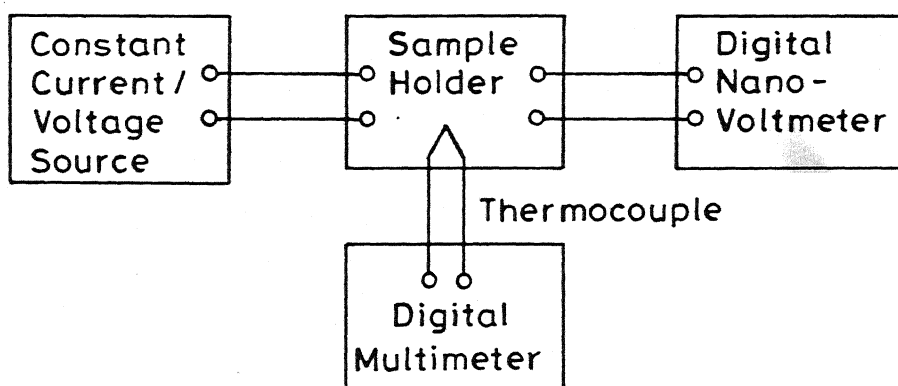
2.3.1 SAMPLE HOLDER

The sample holder suitable for four probe resistivity

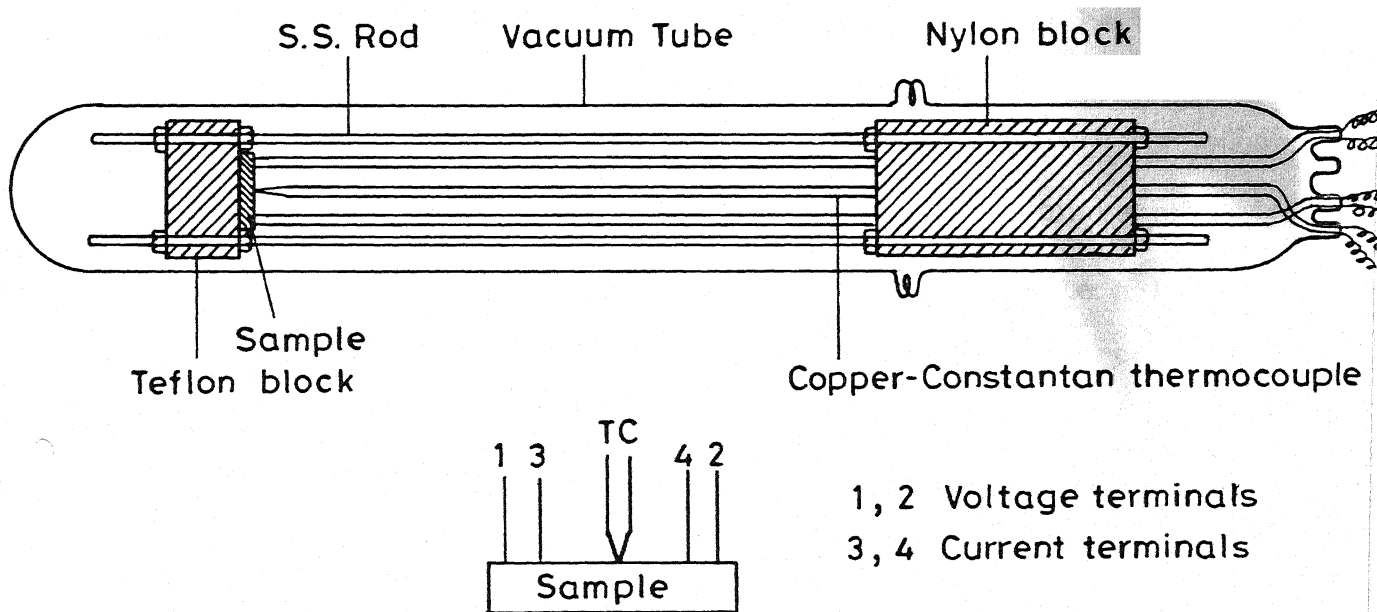
measurement at low temperatures was designed and developed by us, is shown in (Fig. 2.3). It consisted of a Teflon disc (dia ~ 2.43 cm, thickness ~ 1.6 cm), a nylon cylinder (dia ~ 2.43 cm, length ~ 4.76 cm) and two stainless steel (SS) support rods. The SS rods were threaded at both ends, so that above blocks could be held in position with the help of nuts. The entire assembly was inserted into a long quartz tube whose one end was closed and the other end had a flange with "O" ring. This along with another smaller but otherwise similar quartz tube with flange and "O" ring arrangement provide for evacuation of the sample space. The smaller quartz tube had four holes at the end and thus provided for the exit of four electrical lead wires, as well as pair of thermocouple wires.

2.3.2 MEASUREMENT OF RESISTIVITY

The experimental set including the sample holder is shown in (Fig. 2.3). The pellet was first polished with a fine emery paper and then cleaned properly with acetone. Four thin copper wires were soldered onto the one of the flat surfaces of the pellet with silver paint in a rectangular manner. Two of these copper leads were used to pass current and the other two were used to measure the potential difference that developed across these points. The four probes were connected as shown in (Fig. 2.3).



(a)



(b)

(a) Block diagram (b) Sample holder for four terminal resistance measurement at liquid nitrogen temperature.

Fig 2.3

Copper/constantan, i.e. T-type thermocouple placed very close to the sample, measured the temperature of the sample. The reference junction was kept in an oil bath. The two copper wires were taken, one each from the reference and the test junction, were used to measure the thermo emf by means of a digital auto ranging microvoltmeter (Keithley 197 DMM).

The sample holder was housed into a quartz tube which was evacuated upto 10^{-2} torr pressure and then lowered into the Dewar flask. Liquid nitrogen (LN_2) was carefully and slowly poured into the Dewar flask upto the brim. Due to natural evaporation of LN_2 the temperature of the system increased slowly and steadily.. The resistivity was measured by the standard four probe technique between LN_2 and room temperature. The probes were arranged in a square array¹⁹.

To measure the resistivity of the sample a known current (I) was passed from constant current source (Precision, current/voltage source Knick model, West Germany), and corresponding voltage (V) was measured by a digital nanovoltmeter (Keithley 181). The ratio of V/I gave the resistance of the samples which then can be used to calculate the resistivity by knowing the geometry factor of the probe arrangement.

For isotropic parallelepiped type material of major dimensions ℓ_1 , ℓ_2 and ℓ_3 and the four probes on the $\ell_1\ell_2$ face the resistivity ρ was given by Logan et.al.²⁰.

$$\rho = \text{HER}$$

where H was a function of ℓ_2/ℓ_1 . E was an effective thickness and was equal to the actual thickness ℓ_3 when $\ell_3 \ll (\ell_1\ell_2)^{1/2}$, but never much greater than $(\ell_1\ell_2)^{1/2}$. In normalised form $E/(\ell_1\ell_2)^{1/2}$ depended mainly on $\ell_3/(\ell_1\ell_2)^{1/2}$ and was nearly independent of ℓ_2/ℓ_1 over much of the useful range. R is nothing but equal to V/I i.e. ratio of voltage across two probes and the current applied across the other two probes, so knowing R and ℓ_1, ℓ_2, ℓ_3 we could calculate ρ from the above equation.

2.4 MEASUREMENT OF THERMOELECTRIC POWER

2.4.1 SAMPLE HOLDER

Since the measurement of thermoelectric power requires an accurate determination of the temperatures of the two opposite faces of the sample. So the sample holder designing is very important.

The sample holder designed and fabricated locally by us is shown in (Fig. 2.4). It may be divided into three parts. The region one, say the bottom part, consists of two aluminium cylinders which were coated with insulating 'G' varnish (and cured at 423K which is thermally conducting at low temperatures). This cylinder has a central hole and a high purity, (99.99%) copper disc is placed at the top of this and serves as one of the electrodes. A pair of Cu/constantan thermocouple wires are soldered at the back of the Cu-electrode. Another identical

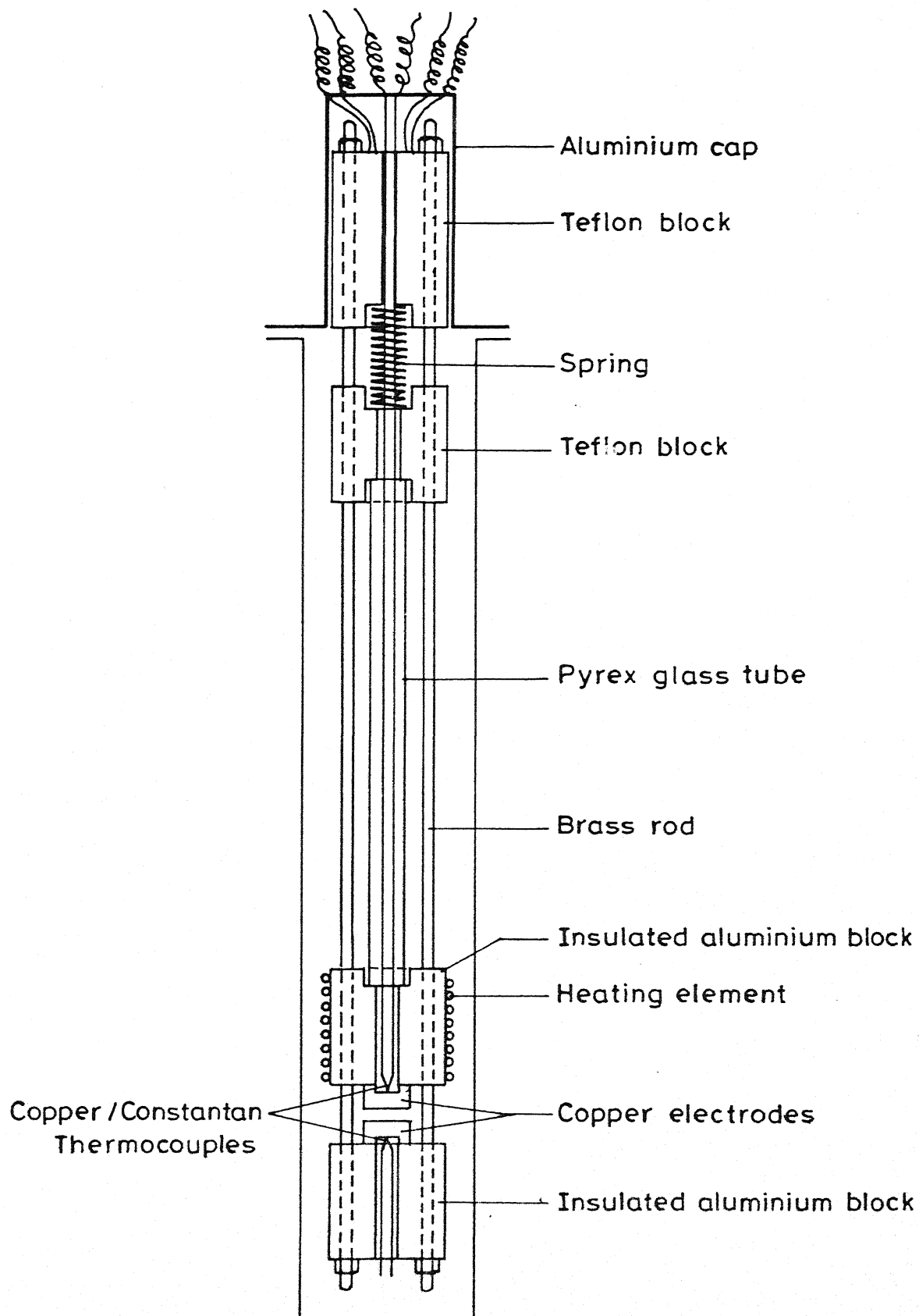
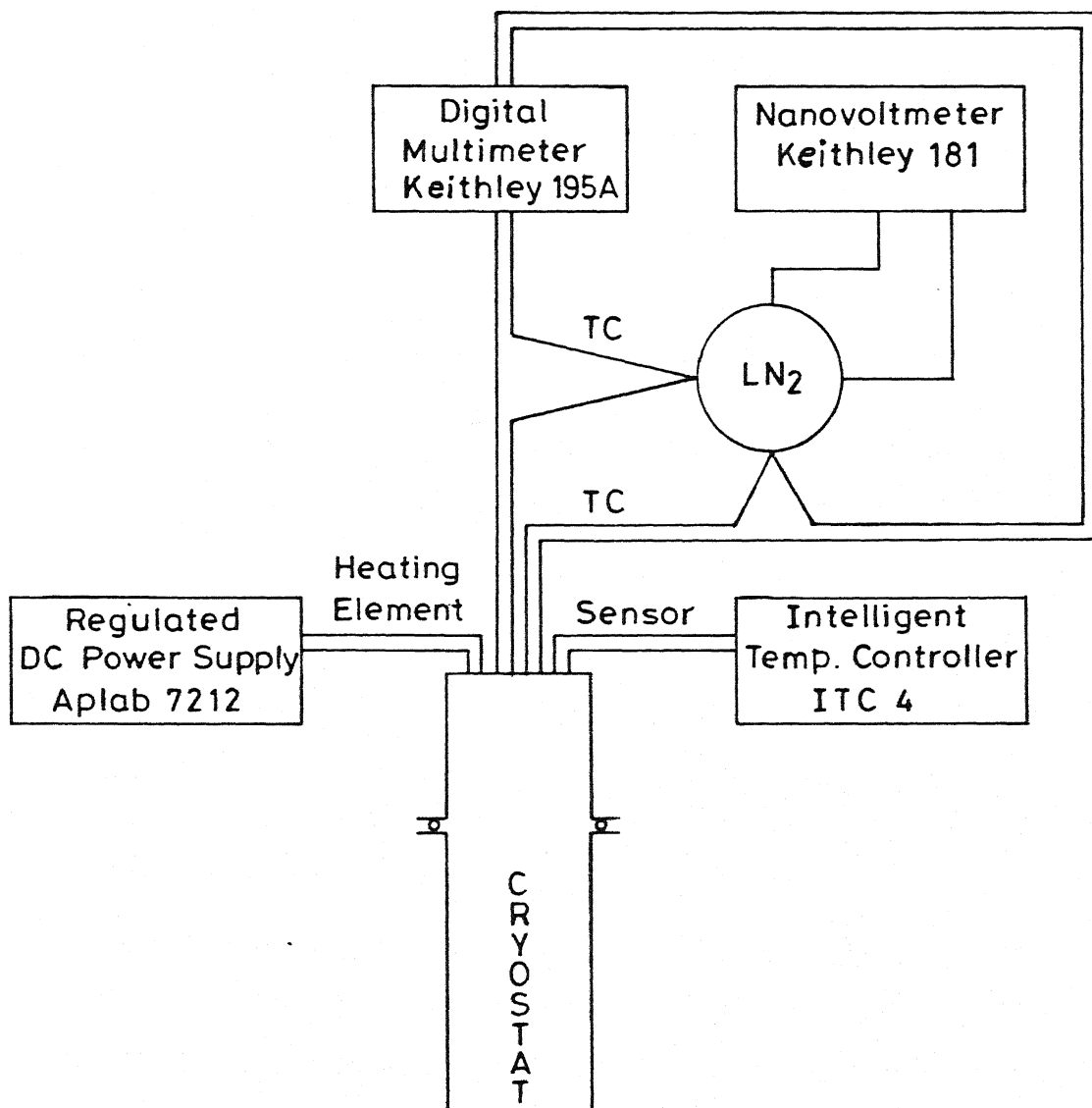


FIG 2.4 Schematic diagram of sample holder for thermoelectric power measurement at liquid nitrogen temperature.

aluminium cylinder which has heating element of special alloy constantan provides the temperature gradient. The sample is pressed between two copper discs backed by the larger aluminium cylinders from the top and bottom.

The intermediate region has a hollow pyrex glass tube seated on the groove of the first regime and aluminium block of the third regime. This is used just to transmit pressure applied to the first regime through spring to make better contact with the pellet.

The third or the other extreme region consists of two Teflon blocks and a spring. The lower Teflon disc is thin and has a groove on both sides. The bottom groove houses the glass tube and the top groove accommodates the spring. The extreme top Teflon cylinder has a groove at the bottom to house the spring. The entire system is assembled with two brass rods threaded at both ends. Nuts are used to fix the whole assembly with the rods. The top Teflon block is housed in a hollow hat type aluminium cylinder. The 'O' ring fits between the hat and the brim of cryostat. This assembly (sample holder) was designed to be compatible with the liquid nitrogen cryostats (Oxford Instruments, Model No. DN1710). The system is made airtight by O-ring and clip arrangement. The thermocouple pairs are taken out from the inside of the cryostat through the holes on the top part of the hat. The holes are then sealed by araldite.



Schematic diagram of thermoelectric power measurement.

Fig 2.5

CENTRAL LIBRARY
I. I. T., KANPUR

Acc. No. **107891**

2.4.2 MEASUREMENT OF THERMOELECTRIC POWER

The samples were thoroughly polished to obtain flat and parallel faces and then cleaned with acetone. Subsequently, conductive silver paint was applied on both faces and cured at room temperature before loading it in the sample holder. The mild spring pressure keeps the sample sandwiched between the two copper electrodes. The sample holder is then lowered into the cryostat and the sample space evacuated upto 10^{-2} torr using a rotary pump (HINDHIVAC VS - 114D). Using a diffusion pump (HINDHIVAC) outer part of the cryostat is evacuated to 10^{-5} torr to minimize heat exchange. An intelligent temperature controller (Oxford Model ITC-4) was used to control the temperature within $\pm 0.1\text{K}$. Liquid nitrogen is gradually poured into the cryostat and at the same time degassing is done to release the inside pressure to avoid accidents.

The gradient heater was powered by a 12V regulated DC power supply (Aplab, 7212). The temperature of the two opposite faces of the sample were measured by a pair of Cu/constantan thermocouple and a digital multimeter (Keithley, 195A). The temperature difference (ΔT) between the two ends was usually kept between (10-15K) except in the critical region where $\Delta T \sim (1-2)\text{K}$ was used. The use of small ΔT became necessary in order to do the measurements in the critical region (78-90K) using liquid nitrogen. The mean temperature of the two ends was taken as the temperature of the sample. The thermoelectric voltage (ΔV) developed across

the sample due to the applied temperature was measured by a nanovoltmeter (Keithley, 181). The copper wires emerging out of the reference junctions (LN_2) of the thermocouples served as the lead wires for the thermoelectric voltage measurement. The thermoelectric power was then calculated as the ratio $\Delta V/\Delta T$. For thermoelectric power sample holder see (Fig. 2.4). The arrangement of experiment is shown in the (Fig. 2.5).

CHAPTER 3

3. RESULTS AND DISCUSSION

3.1 MATERIALS SYNTHESIS

For preparation of $\text{SmBa}_2\text{Cu}_3\text{O}_{7-\delta}$ samples, appropriate amounts of Sm_2O_3 , BaCO_3 and CuO were weighed and homogenized in a pestle and mortar followed by pelletization. Two sets of samples were prepared following two different routes. The samples prepared by the first route (see the flow chart 1) are referred to as A_1 and those by the second route by A_2 respectively. In case of A_1 samples the reaction temperature was 1173 K (12-16 hours), the sintering temperature (T_s) was $\sim 1198\text{K}$ (~ 20 hrs). While these temperatures for A_2 samples were 1198K and 1223K respectively. Both A_1 and A_2 samples were sintered twice at their respective sintering temperatures and also soaked at the same temperature of $\sim 833\text{K}$ for ~ 10 hrs. These samples were subsequently used for XRD, resistivity and thermoelectric power studies.

To prepare the Ca-doped Sm-Ba-Cu-O samples, a similar heat schedule as above was followed. The doped samples prepared via the first route are referred to as B_1 and those via the second route as B_2 (see Flow chart 2).

All samples that are pure Sm-Ba-Cu-O (A_1 and A_2) as well as Ca-doped Sm-Ba-Cu-O (B_1 and B_2) were prepared under a continuous flow of oxygen during reaction, sintering and soaking. In all sixteen samples were prepared, four each of A_1 , A_2 , B_1 and B_2 , and investigated. The results presented and discussed in this chapter are representative of the best samples.

Two different heating schedules were mainly used to optimize the preparational conditions. As discussed later, the samples prepared via the second rate ($T_R = 1198K$, $T_S = 1223K$) yielded better properties such as lower room temperature resistivity, thermoelectric power and a bit higher T_c .

3.2 MATERIAL CHARACTERIZATION BY XRD

A number of samples of each type i.e. A_1 and A_2 ($SmBa_2Cu_3O_{7-\delta}$) and B_1 and B_2 ($SmBa_{1.5}Ca_{0.5}O_{7-\delta}$) were examined by X-ray diffraction (XRD) at two different scanning speeds (1.2 and $0.3^\circ/\text{min}$) at room temperature. The results are shown in Figs. 3.1 to 3.4 corresponding to a scanning speed of $1.2^\circ/\text{min}$ for A_1 , A_2 , B_1 and B_2 respectively.

It should be pointed out that $SmBa_2Cu_3O_{7-\delta}$ is isostructural to the well known $YBaCu_3O_{7-\delta}$ high T_c superconductor which has an orthorhombic structure with $a = 3.815\text{\AA}$, $b = 3.891\text{\AA}$, $c = 11.673\text{\AA}$. The former, i.e., Sm-based HTSC has a T_c of $88.1K^{21}$ while the

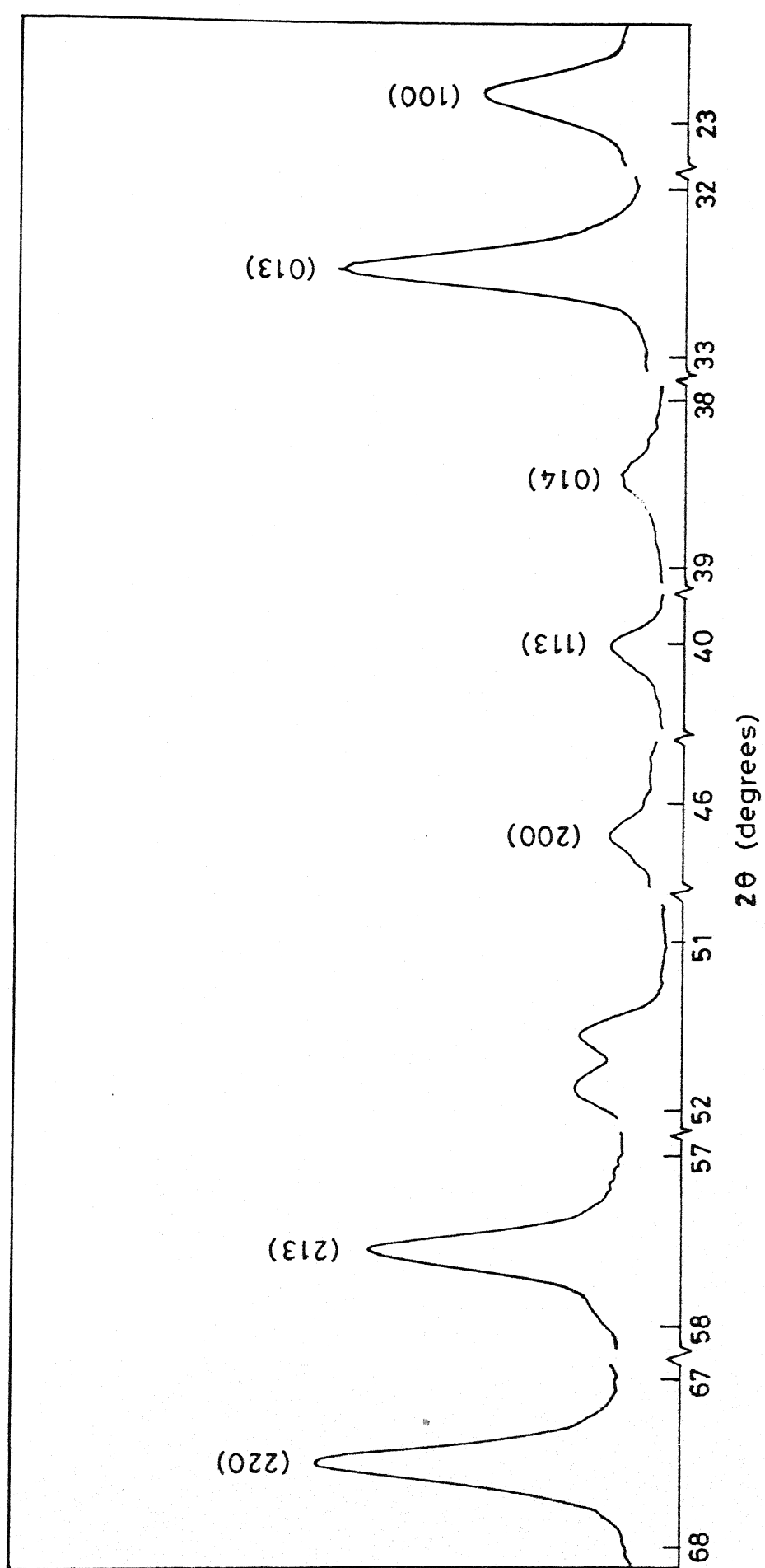


Fig. 3.1 X-ray diffraction pattern for $\text{SmBa}_2\text{Cu}_3\text{O}_{7-\delta}$

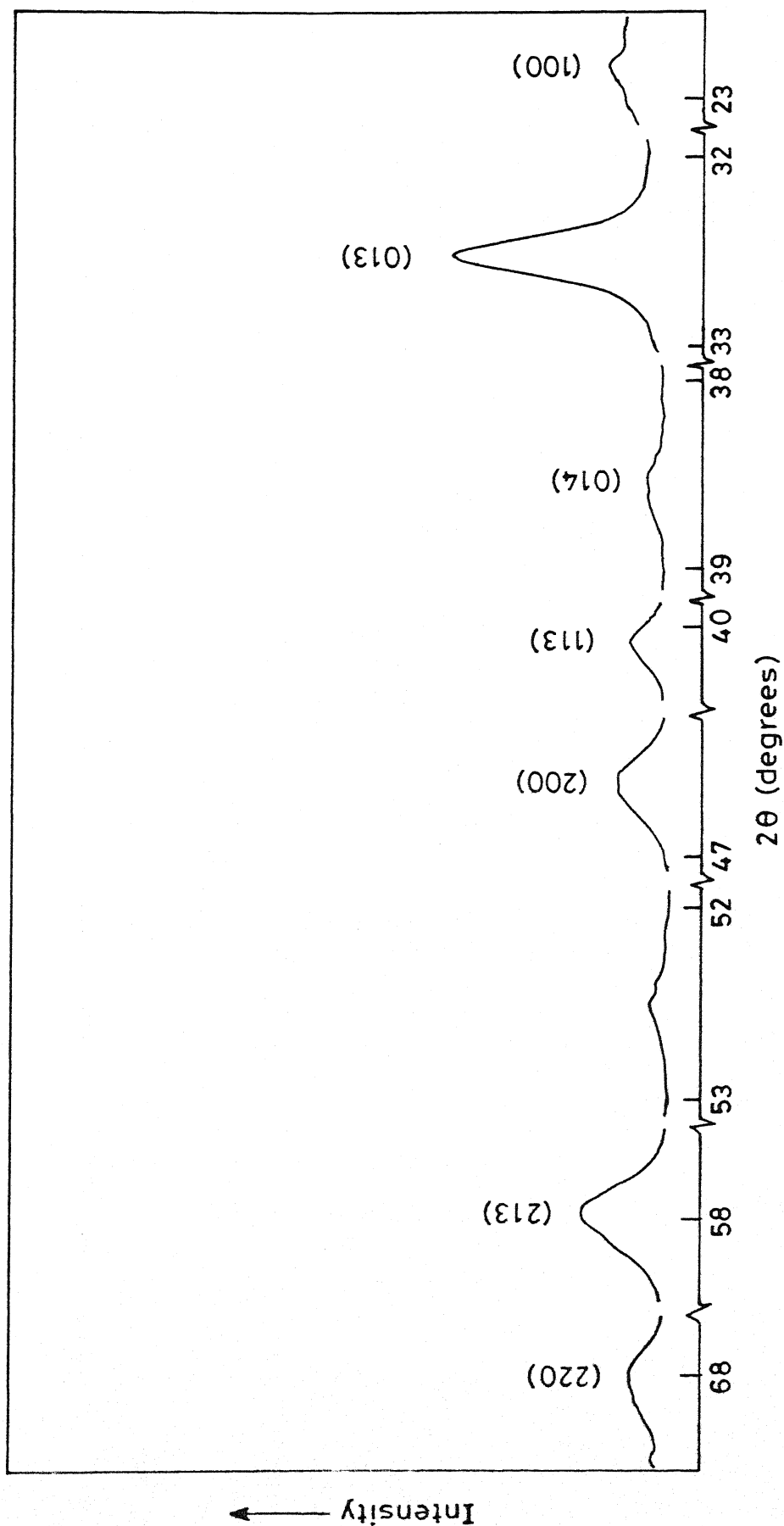


Fig. 3.2 X-ray diffraction pattern for $\text{SmBa}_2\text{Cu}_3\text{O}_{7-\delta}$

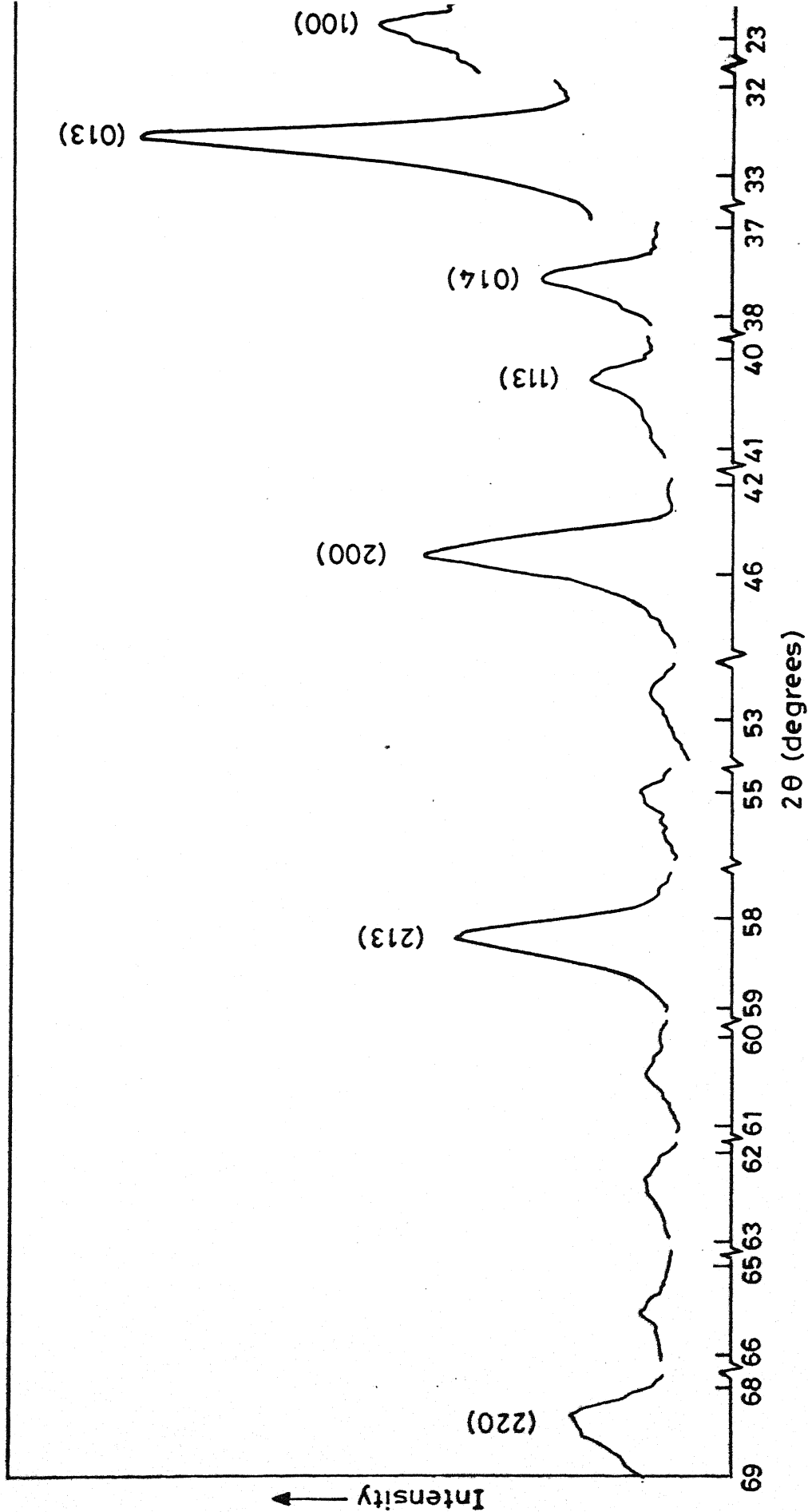


Fig.3.3 X-ray diffraction pattern for $\text{SmBa}_{1.5}\text{Ca}_{0.5}\text{Cu}_3\text{O}_{7-\delta}$

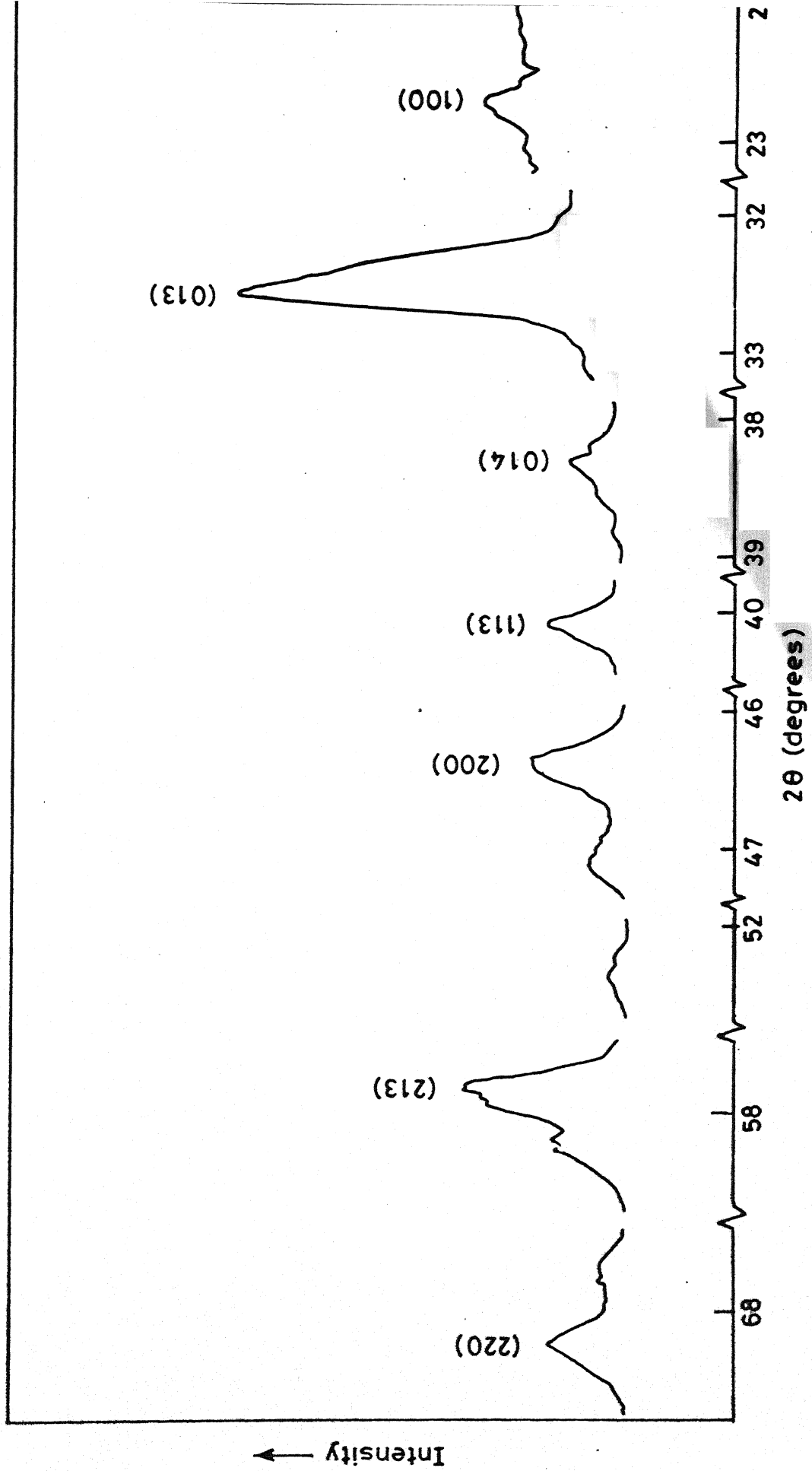


Fig. 3.4 X-ray diffraction pattern for $\text{SmBa}_{1.5}\text{Ca}_{0.5}\text{Cu}_3\text{O}_{7-\delta}$

TABLE 1.1

XRD BY CuK_α WITH MONO CHROMATOR

$\text{SmBa}_2\text{Cu}_3\text{O}_{7-\delta}$ (Figs.3.1 and 3.2)

Current	20 mA
Voltage	30 KV
Time constant	10 second
Scan speed	$1.2^\circ/\text{min}$
Chart speed	30 mm/min
Full scale intensity	200 counts/min

$\text{SmBa}_{1.5}\text{Ca}_{0.5}\text{Cu}_3\text{O}_{7-\delta}$ (Figs.3.3 and 3.4)

Current	20 mA
Voltage	30 KV
Time constant	10 second
Scan speed	$1.2^\circ/\text{min}$
Chart speed	30 mm/min
Full scale intensity	10K counts/min

40

FLOW CHART 1

PREPARATIONAL SCHEDULE OF $\text{SmBa}_2\text{Cu}_3\text{O}_{7-\delta}$

SAMPLES A

↓
 $\text{Sm}_2\text{O}_3, \text{BaCO}_3, \text{CuO}$
↓

Weighing
↓

Homogenisation
↓

Pressing (~ 3 ton cm^{-2})
↓

(Sample A_1) (Sample A_2)
↓

Reaction 1173 K
(12-16) hrs
↓

Pulverizing
↓

Pressing (~ 5 ton cm^{-2})
↓

Sintering (1198 K)
(20 hrs, 2 times)
↓

Soaking (833 K)
(10 hrs)

↓
Reaction 1198 K
(12-16) hrs
↓

Pulverizing
↓

Pressing (~ 5 ton cm^{-2})
↓

Sintering (1223 K)
(20 hrs, 2 times)
↓

Soaking (833 K)
(10 hrs)

FLOW CHART 2PREPARATIONAL SCHEDULE OF $\text{SmBa}_{1.5}\text{Ca}_{0.5}\text{Cu}_3\text{O}_{7-\delta}$ SAMPLES B

Sm_2O_3 , BaCO_3 , CaCO_3 , CuO

↓
Weighing

↓
Homogenization

↓
Pressing ($\sim 3 \text{ ton cm}^{-2}$)

(Sample B₁) (Sample B₂)

↓
Reaction 1173 K
(12-16) hrs

↓
Reaction 1198 K
(12-16) hrs

↓
Pulverizing

↓
Pulverizing

↓
Pressing ($\sim 5 \text{ ton cm}^{-2}$)

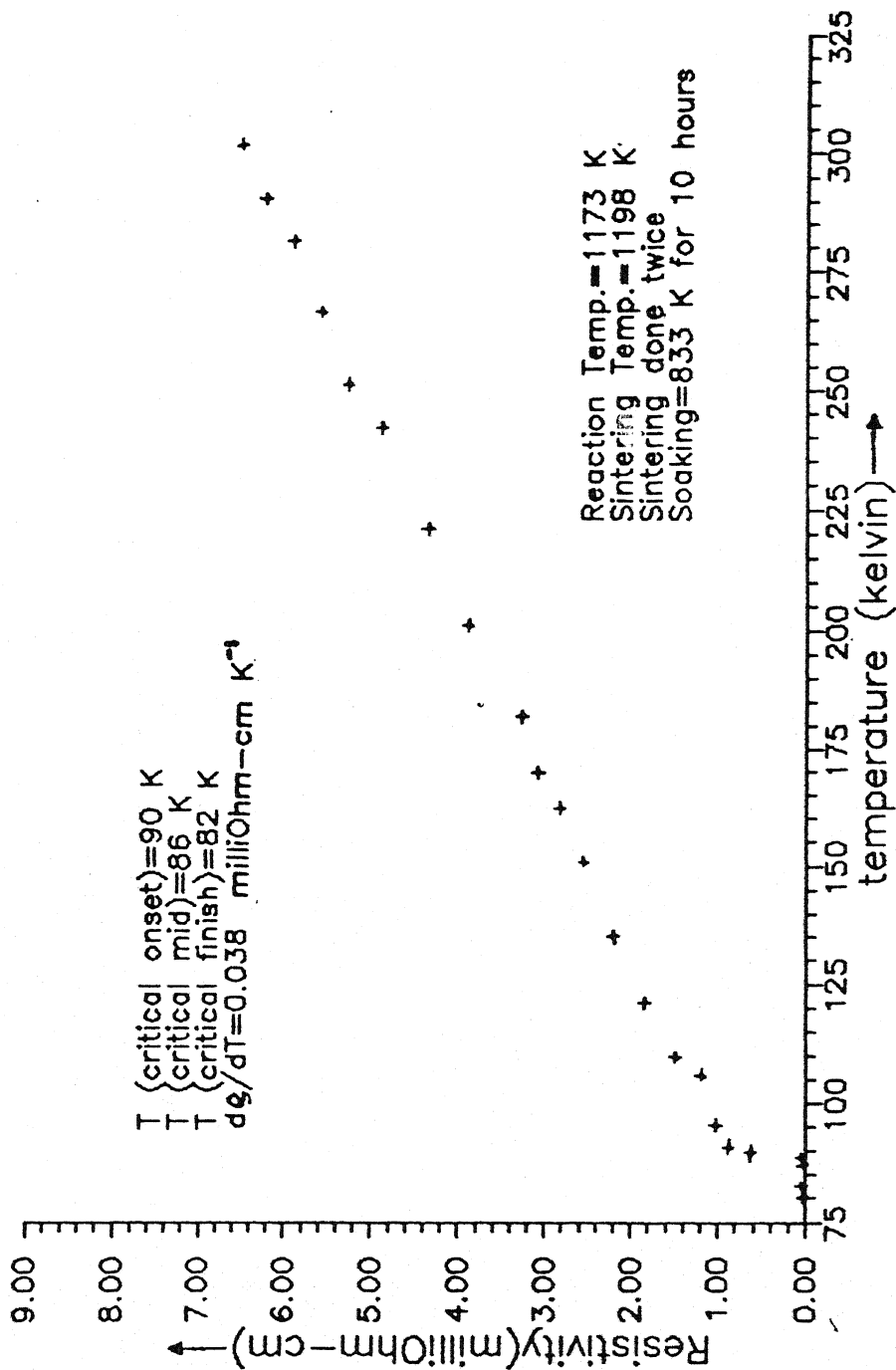
↓
Pressing ($\sim 5 \text{ ton cm}^{-2}$)

↓
Sintering (1198 K)
(20 hrs, 2 times)

↓
Sintering (1223 K)
(20 hrs, 2 times)

↓
Soaking (833 K)
(10 hrs)

↓
Soaking (833 K)
(10 hrs)



System : Sm Ba₂ Cu₃ O_{7-s} (A₁)

Fig: 3.5

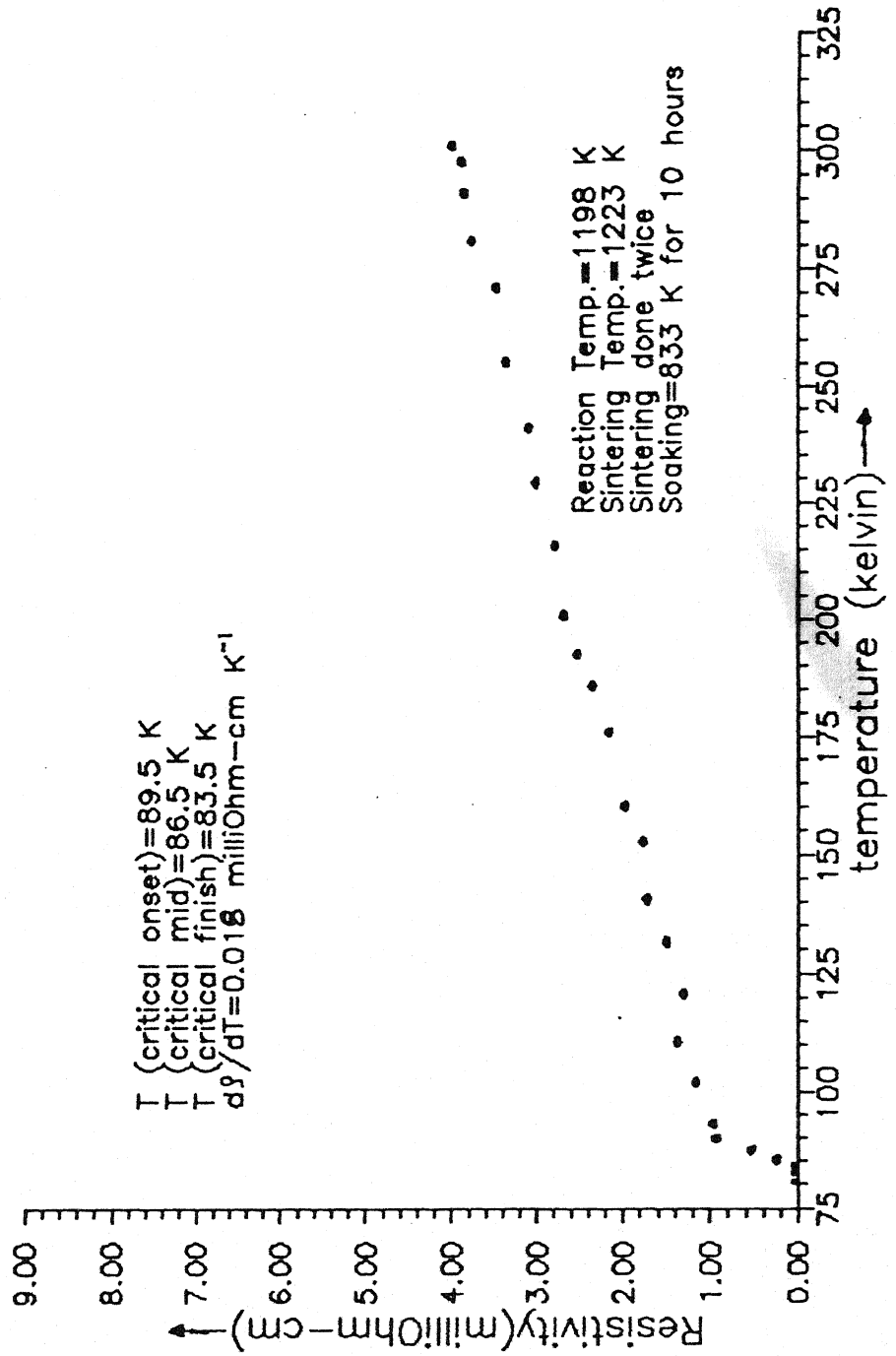
latter, i.e. Y-based HTSC, has a T_c of 94 K^{22} . Even though YBaCuO has a somewhat higher T_c it is very difficult to prepare the same as a single phase material. As our XRD results (Figs. 3.1 to 3.4) reveal, $\text{SmBa}_2\text{Cu}_3\text{O}_{7-\delta}$ as well as $\text{SmBa}_{1.5}\text{Ca}_{0.5}\text{O}_{7-\delta}$ are all single phase materials.

3.2.1 PURE $\text{SmBa}_2\text{Cu}_3\text{O}_{7-\delta}$ (A_1 , A_2 SAMPLES)

The XRD patterns of A_1 and A_2 samples are shown in Figs. 3.1 and 3.2. The diffraction patterns for these two samples are similar except that the patterns (Fig. 3.1) for A_1 samples ($T_R = 1173\text{K}$ and $T_S = 1198\text{K}$) show a double peak at $2\theta \leq 51.5^\circ$ which is not present in the XRD pattern of A_2 samples prepared at $T_R = 1198\text{K}$ and sintered at $T_S = 1223\text{K}$. This additional peak in XRD pattern of A_1 samples may be attributed to the presence of a second unreacted phase which has disappeared in A_2 samples. This is likely because A_2 samples were prepared and sintered at a higher temperature.

3.2.2 Ca-DOPED B_1 , B_2 SAMPLES ($\text{SmBa}_{1.5}\text{Ca}_{0.5}\text{Cu}_3\text{O}_{7-\delta}$)

Figures 3.3 and 3.4 show the XRD patterns of Ca-doped samples ($\text{SmBa}_{1.5}\text{Ca}_{0.5}\text{O}_{7-\delta}$), B_1 and B_2 respectively. The results show that the doped samples $\text{SmBa}_{1.5}\text{Ca}_{0.5}\text{O}_{7-\delta}$ (both B_1 and B_2) are single phase material. A comparison of Fig. 3.2 (pure A_2 sample) and Fig. 3.4 (Ca-doped B_2 sample) would suggest that the patterns are essentially similar except that all the peaks of Ca-doped sample have shifted to a somewhat higher 2θ



System : Sm Ba₂Cu₃O_{7-δ}

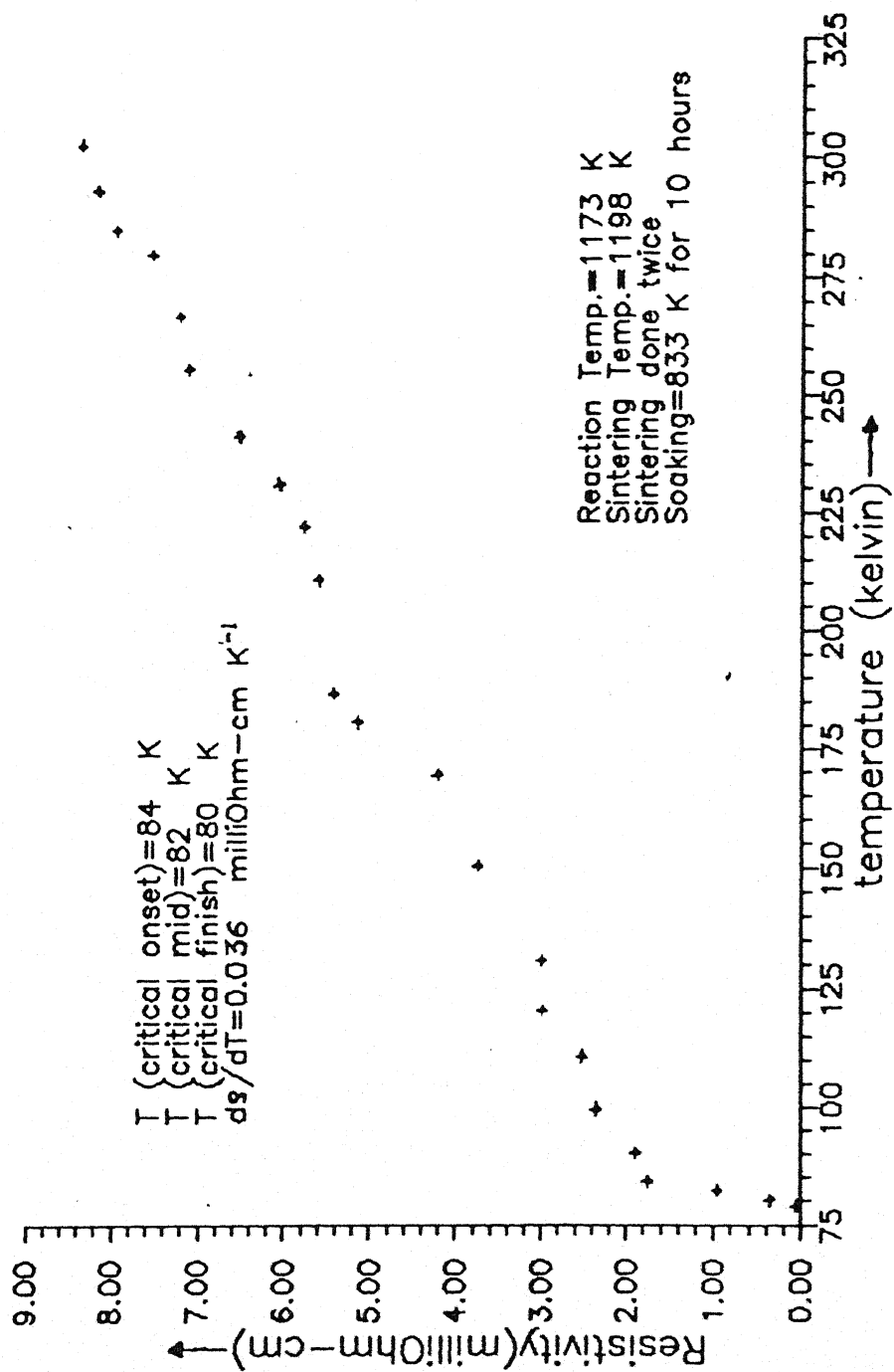
values. This is expected in view of the fact that the size of Ca^{++} is smaller than that of the host Ba^{++} which would decrease the lattice parameter 'a' and $a \propto d$, so 'd' value is decreased. This in turn increases the θ value (d is inversely proportional to $\sin\theta$). So shifting of peak to higher θ is quite in agreement with the expected one.

3.3 ELECTRICAL RESISTIVITY MEASUREMENT

3.3.1 PURE $\text{SmBa}_2\text{Cu}_3\text{O}_{7-\delta}$ (A_1-A_2) SAMPLES)

The resistivity for each sample was measured between room temperature and LN_2 temperature (Fig. 3.5) shows the resistivity as a function of temperature for the sample prepared via the first route ($T_R = 1173\text{K}$, $T_S = 1198\text{K}$). The resistivity vs. temperature plot shows a critical onset temperature (T_{co}) of 90K, critical mid temperature (T_{cm}) of 86K, and critical finish temperature (T_{cf}) of 82K. The resistivity with respect to temperature, i.e. $\frac{d\rho}{dT} \approx 0.03 \text{ m Ohm cmK}^{-1}$ over the entire temperature range above T_c . The room temperature resistivity $\rho_{RT} \approx 6.5 \text{ m Ohm cm}$. The resistivity at critical onset temperature $\rho_{T_{Co}} \approx 0.8 \text{ m Ohm-cm}$. The resistivity at $T < T_c$ could not be measured but is expected to be less than $\sim 10^{-3} \text{ mOhm-cm}$. This limitation was because of the fact that the resolution of monovoltmeter was 10 nV and the maximum current that could be drawn from the current source was of the order of several tens of mA.

Figure 3.6 shows the similar results (ρ vs. T) for A_2 sample which was processed at higher temperatures. For this



System : $\text{SmBa}_{1.5}\text{CaCu}_3\text{O}_{7-\delta}$
 FIG. 37 (B_1)

sample $T_{co} = 89.5$ K, $T_{cm} = 86.5$ K, $T_{cf} = 83.5$ K, $\rho_{RT} \simeq 4$ m. Ohm cm, $\rho_{T_{co}} \simeq 1$ m Ohm.cm, and $d\rho/dT = 0.018$ m Ohm cm K^{-1} .

3.3.2 Ca DOPED $SmBa_2Cu_3O_{7-\delta}$ (B_1 - B_2 SAMPLES), $SmBa_{1.5}Ca_{0.5}Cu_3O_{7-\delta}$

The resistivity for each sample was measured between room temperature and LN_2 temperature (Fig. 3.7) shows the resistivity as a function of temperature for the sample prepared via the first route ($T_P = 1173$ K, $T_S = 1198$ K). The resistivity vs. temperature plot shows a critical onset temperature (T_{co}) of 84K, critical mid temperature (T_{cm}) of 82K, and critical finish temperature (T_{cf}) of 80K. The resistivity with respect to temperature, i.e. $d\rho/dT \simeq 0.036$ mOhmcm K^{-1} over the entire temperature range above T_c . The room temperature resistivity $\rho_{RT} \simeq 8.38$ m Ohm cm. The resistivity at critical onset temperature $\rho_{T_{co}} \simeq 1.8$ m Ohm-cm. The resistivity at $T < T_c$ could not be measured but is expected to be less than $\sim 10^{-3}$ mOhmcm. This limitation was because of the fact that the resolution of nanovoltmeter was 10 nV and the maximum current that could be drawn from the current source was of the order of several tens of mA.

Figure 3.8 shows the similar results (ρ vs. T) for B_2 sample which was processed at higher temperatures. For this sample $T_{co} = 86$ K, $T_{cm} = 83$ K, $T_{cf} = 80$ K, $\rho_{RT} \simeq 7.56$ mOhm cm, $\rho_{T_{co}} \simeq 1.2$ mOhm.cm, and $d\rho/dT = 0.034$ mOhm cm K^{-1} .

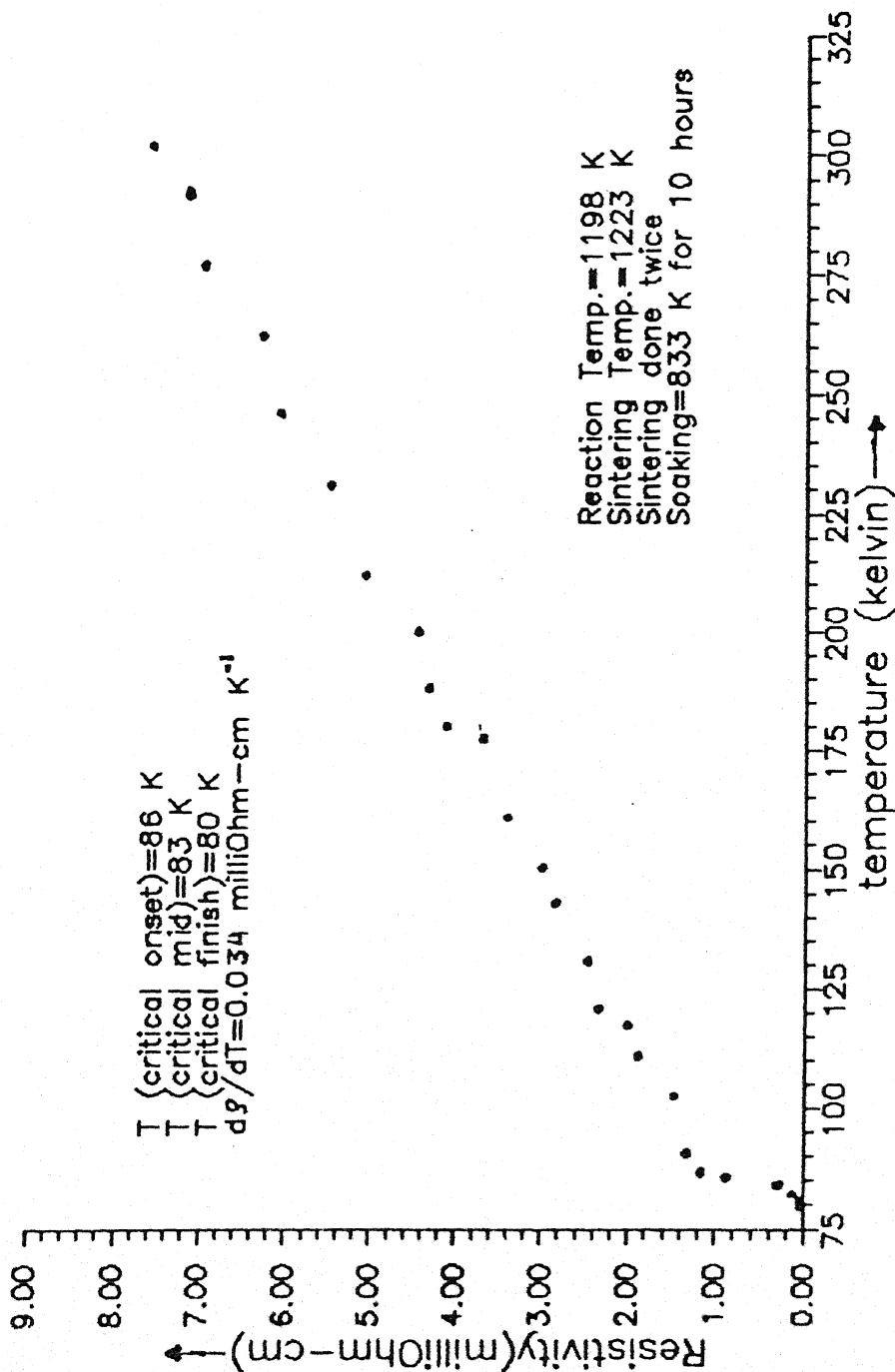
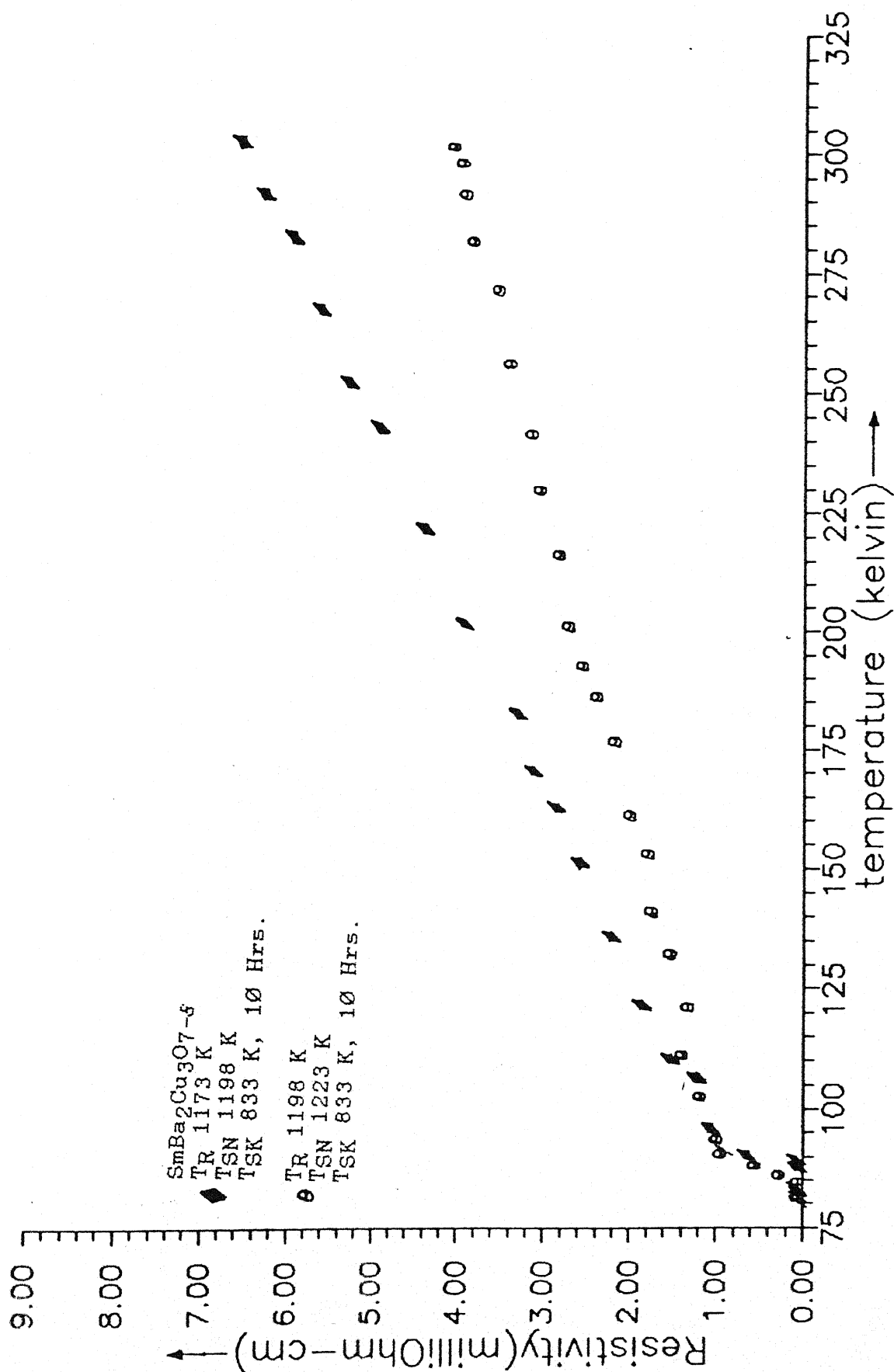


FIG. 3.8 System : $\text{Sm Bq}_{1.5}\text{CaCu}_3\text{O}_{7.6}$ (B_2)

FIG. 3.9, (A_1 - A_2)

3.3.3 THE EFFECT OF HEAT TREATMENT

SmBa₂Cu₃O_{7-δ} (A₁ to A₂ Samples)

The electrical resistivity (ρ) of the two samples, A₁ and A₂ prepared and processed at lower and higher temperatures respectively, is compared in Fig. 3.9. It is noted that the A₂ sample which was heat treated at somewhat higher temperatures shows better properties compared to the A₁ samples. For instance A₂ sample has $\rho_{RT} = 4.00$ mOhmcm, $\rho_{T_{Co}} = 1$ mOhmcm, $T_{Co} = 89.5$ K and $d\rho/dT = 0.018$ mOhmcm K⁻¹ while A₁ sample has $\rho_{RT} = 6.5$ mOhm, $\rho_{T_{Co}} = 0.8$ mOhm, $T_{Co} = 90$ K and $d\rho/dT = 0.03$ mOhm cm K⁻¹. Thus the ρ_{RT} of A₂ is 61.5% lower than that of A₁ sample. These results are consistent with XRD data which also suggest that the sample prepared and processed at higher temperatures did not show extra peaks.

SmBa_{1.5}Co_{0.5}Cu₃O_{7-δ} (B₁ and B₂ Samples)

The effect of heat treatment for Ca-doped Sm-Ba-Cu-O materials is similar (Fig. 3.10) to that (Fig. 3.9) observed for pure Sm-Ba-Cu-O samples, i.e. B₂ samples which were treated at higher temperatures show better superconducting properties than the B₁ samples. For B₂ sample; $\rho_{RT} = 7.56$ mOhm cm, $\rho_{T_{Co}} = 1.2$ mOhm cm, $T_{Co} = 86$ K and $d\rho/dT = 0.034$ mOhmcmK⁻¹ while these figures for B₁ samples are $\rho_{RT} = 8.38$ m Ohm cm, $\rho_{T_{Co}} = 1.8$ m Ohm cm, $T_{Co} = 84$ K and $d\rho/dT = 0.036$ m Ohm cmK⁻¹ respectively.

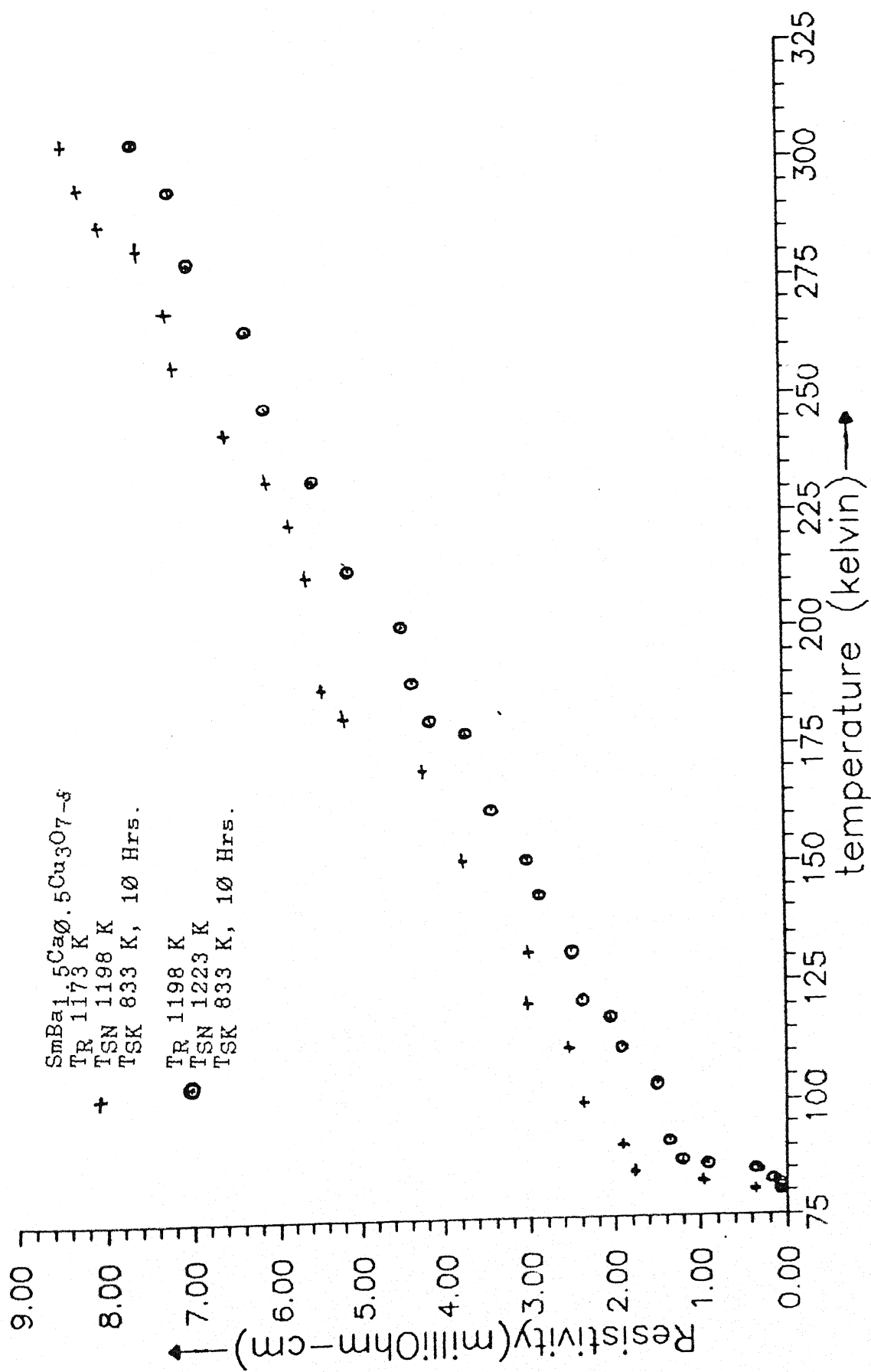


FIG 310 (B₁-B₂)

3.3.4 THE EFFECT OF DOPING

The effect of partial (25%) substitution of Ca for Ba in Sm-Ba-Cu-O system is not very favourable. The critical onset temperature T_{co} is lowered and the room temperature resistivity ρ_{RT} is increased for both the doped samples B_1 and B_2 (Fig. 3.10).

3.3.5 COMBINED EFFECT OF HEAT TREATMENT AND DOPING

The electrical resistivity of all the four samples, pure $\text{SmBa}_2\text{Cu}_3\text{O}_{7-\delta}$ (A_1 and A_2) and Ca-doped $\text{SmBa}_{1.5}\text{Ca}_{0.5}\text{Cu}_3\text{O}_{7-\delta}$ (B_1 and B_2), as a function of temperature is shown in (Fig. 3.11).

A summary of the comparative studies is given below:

- (a) The sample which is not doped and heat treated at higher temperature has lower ρ_{RT} and higher T_c .
- (b) The sample which is not doped but heat treated at relatively lower temperature than that of (a), has higher ρ_{RT} and lower T_c than that of (a).
- (c) The sample which is Ca-doped partially in place of Ba and heat treated identically as in (a), has still higher ρ_{RT} and lower T_c than those in (b).
- (d) The sample which is Ca-doped partially in place of Ba and heat treated identically as (b) has highest ρ_{RT} and lowest T_c of all.

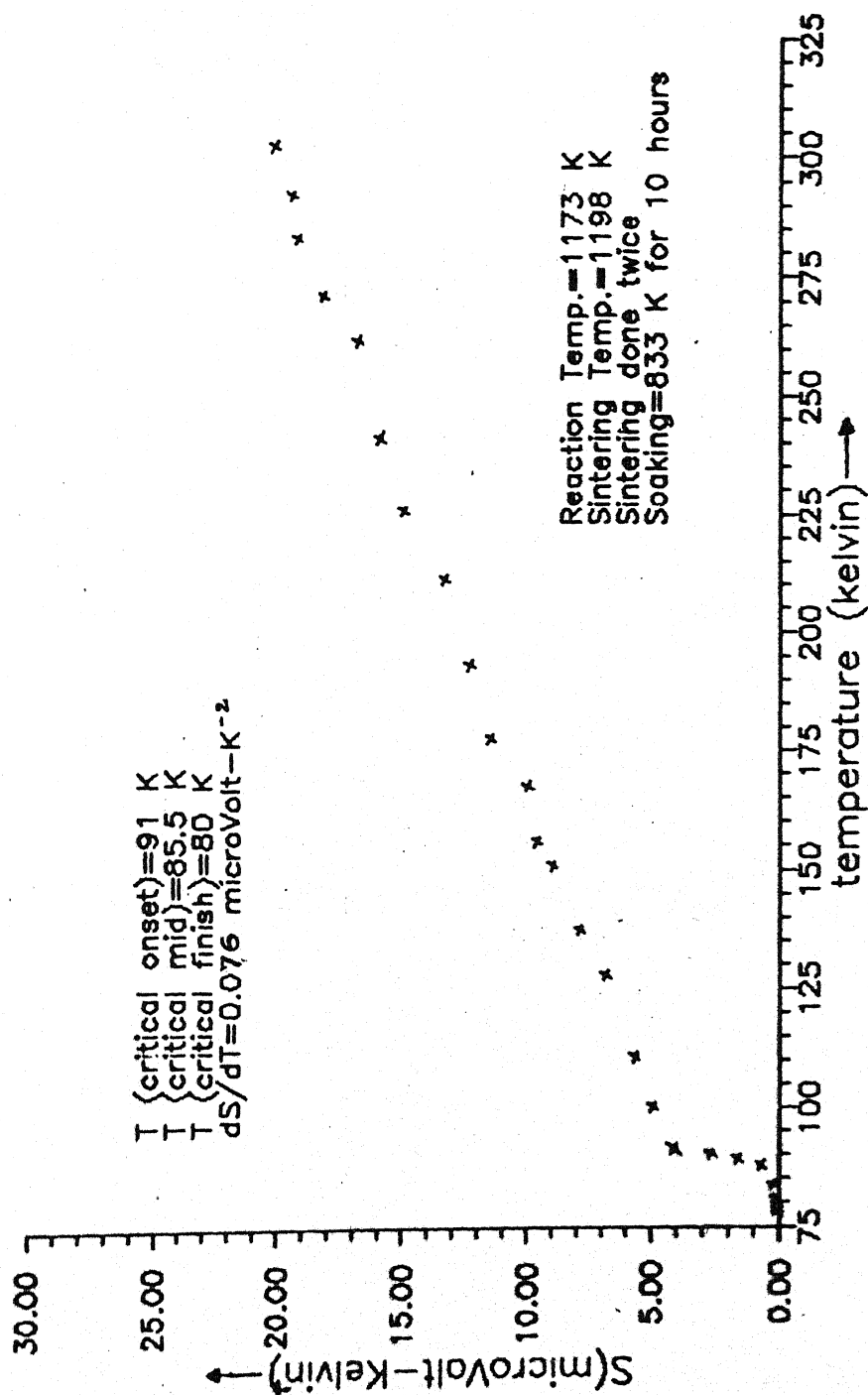
So doping of Ca in place of Ba in Sm-Ba-Cu-O system and insufficient heat treatment necessarily enhances ρ_{RT} and lowers the T_c value to some extent.

3.4 THERMOELECTRIC POWER

When a temperature difference (ΔT) is applied across a sample, i.e. one end is hotter than the other end, a thermo emf (ΔV) is induced and the ratio $\Delta V/\Delta T$ is defined as the thermo electric power,

$$S = \lim_{T \rightarrow 0} \left(\frac{\Delta V}{\Delta T} \right)$$

The measurement of thermoelectric power is an important tool to determine the nature of charge carriers. In addition, it provides, in combination with resistivity studies, useful information regarding the transport properties. The application of a temperature difference across the sample disturbs the electron/hole equilibrium distribution function, and forces the flow of charge carriers until a new equilibrium state is reached, resulting in a potential difference across the sample. In general, both the carrier concentration and their mobility at the two ends differ, and thus there is a flow of carriers from hot end to cold end. The cold end being at a higher potential than the hot end would mean that the majority carriers are holes, otherwise would suggest electrons. The sign



System : $\text{SmBa}_2\text{Cu}_3\text{O}_{7-\delta}$ (A_1)

FIG. 3.12

convention is that if the cold end is negative/positive with respect to the hot end, the thermo electric power is taken as negative/positive.

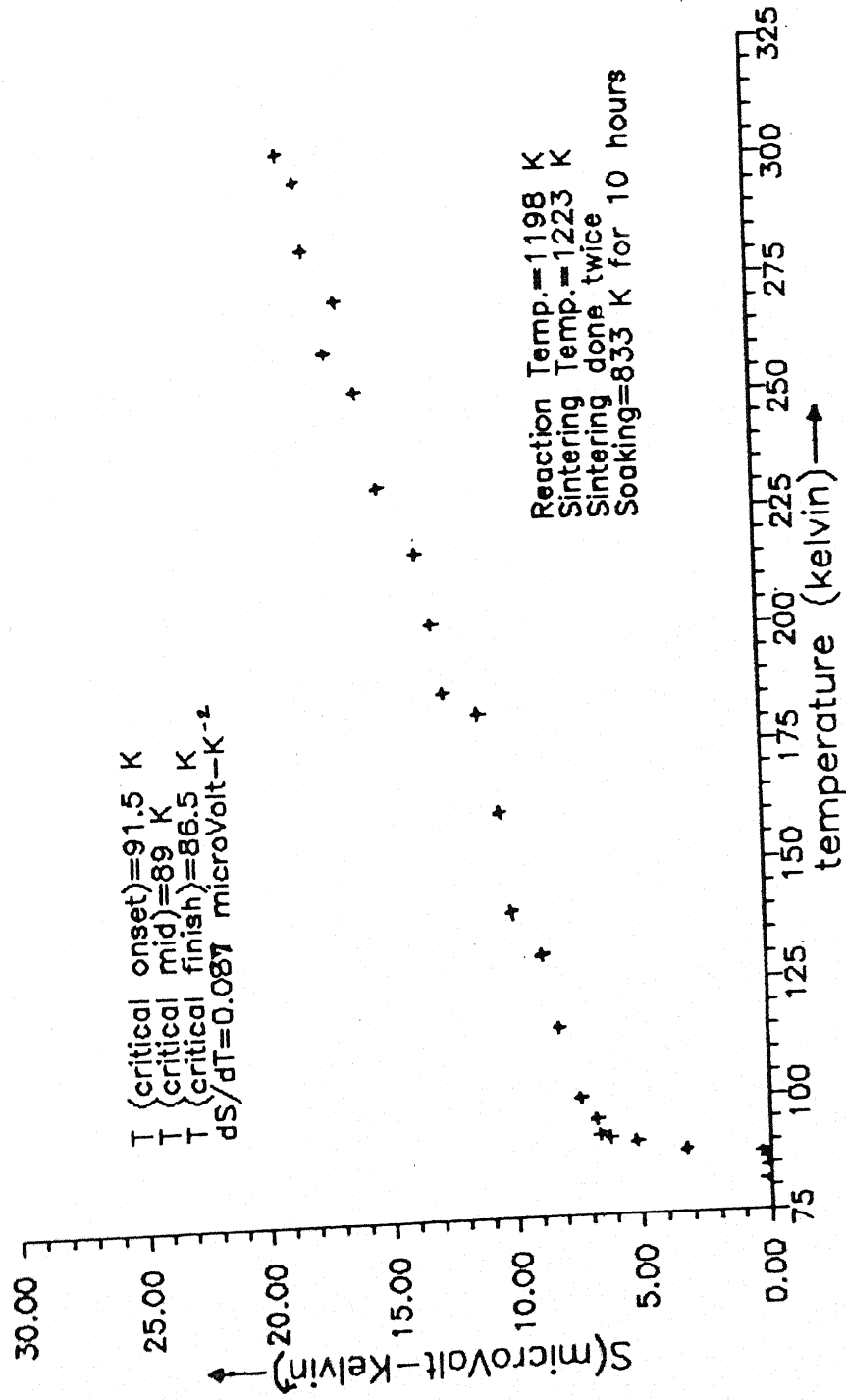
Thermoelectric power is sensitive to structural defects, and hence the samples must be carefully processed. In general, any thing which increases the conductivity (or decreases the resistivity) such as reduced thermal vibrations on cooling the specimen or decrease in the concentration of impurities, tends to decrease the thermo electric power. Thus it is only to be expected that the thermo electric power be zero in a superconductor. By and long, most superconductors below T_c show no thermo electric power.

3.4.1 THERMO ELECTRIC POWER OF PURE $\text{SmBa}_2\text{Cu}_3\text{O}_{7-\delta}$

Figures 3.12 and 3.13 show the thermo electric power (s) of $\text{SmBa}_2\text{Cu}_3\text{O}_{7-\delta}$ samples prepared and processed at two different temperatures (A_1 and A_2) as a function of temperature between LN_2 and room temperature.

A_1 sample has $S \approx 20 \mu\text{V K}^{-1}$ at 300K, and $\sim 4 \mu\text{V K}^{-1}$ at T_{c0} . The thermo electric power decreases linearly as the temperature decreases, and it drops suddenly to zero value at the critical temperature ($T_c = 85.5 \text{ K}$). The slope of the S vs. T curve, $dS/dT \approx 0.076 \mu\text{V K}^{-2}$.

The positive sign of thermo electric power suggests that the charge carrier are holes in this material.



System : Sm Ba₂ Cu₃ O_{7-s} (A₂)

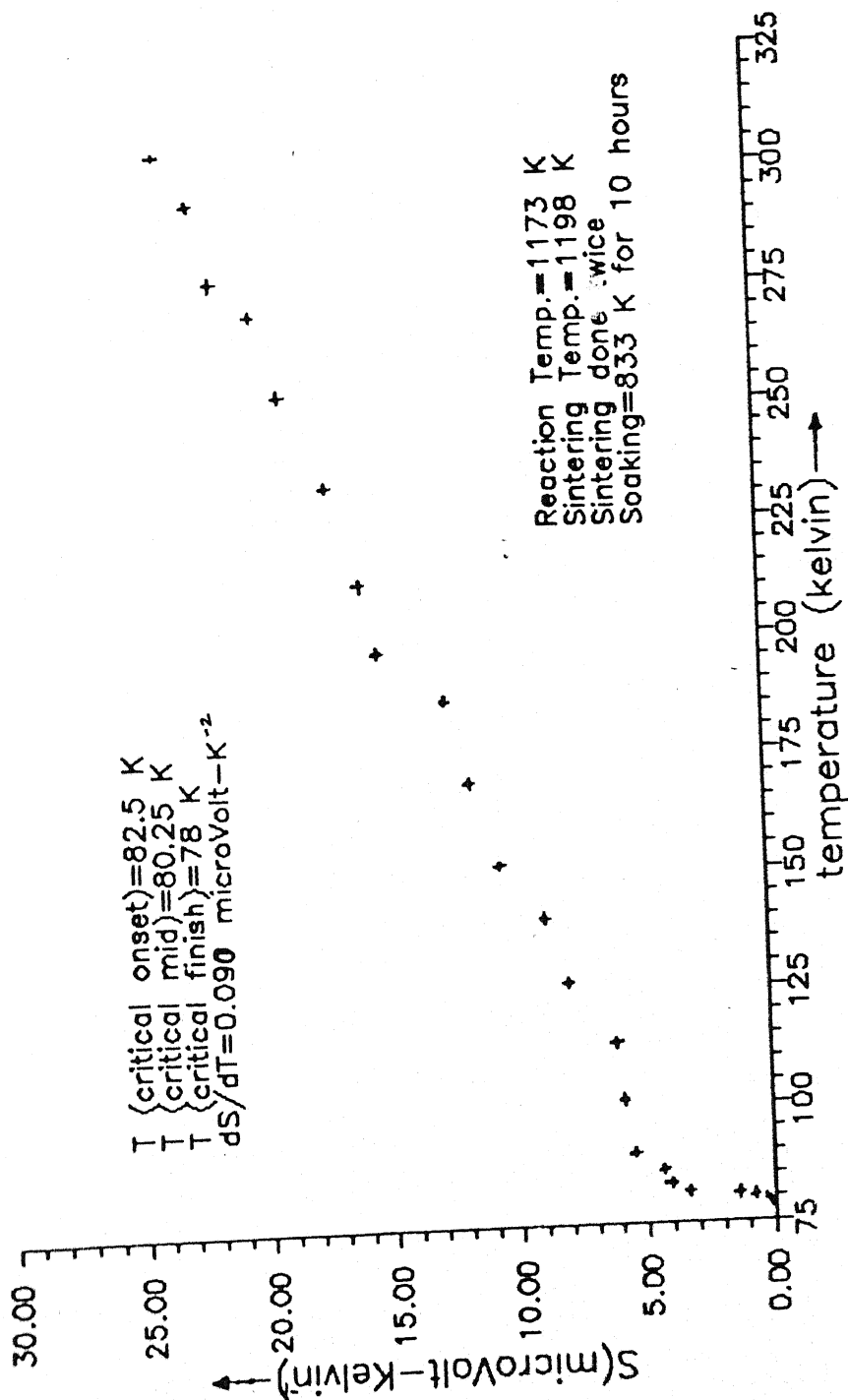
FIG.3.13

TABLE 2

	SmBa ₂ Cu ₃ O _{7-δ}	SmBa _{1.5} Ca _{0.5} Cu ₃ O _{7-δ}	YBa ₂ Cu ₃ O _{7-δ} ⁽²²⁾ (Slowly cooled in oxygen)
	A ₂	B ₂	
T _{Co} [*] (K)	89.5	86	95.5
T _{cm} [*] (K)	86.5	83	94
T _{cf} [*] (K)	83.5	80	92.2
ρ _{RT} [*] (milli Ohmcm)	4.0	7.56	~1.3
ρ _{TCo} [*] (milli Ohm cm)	1	1.2	~0.42
$\frac{d\rho}{dT}$ (milli OhmcmK ⁻¹)	0.018	0.034	0.004
S _{RT} (μV K ⁻¹)	18.6	22	(-2.7)
$\frac{dS}{dT}$ (μV K ⁻²)	0.062	0.081	~

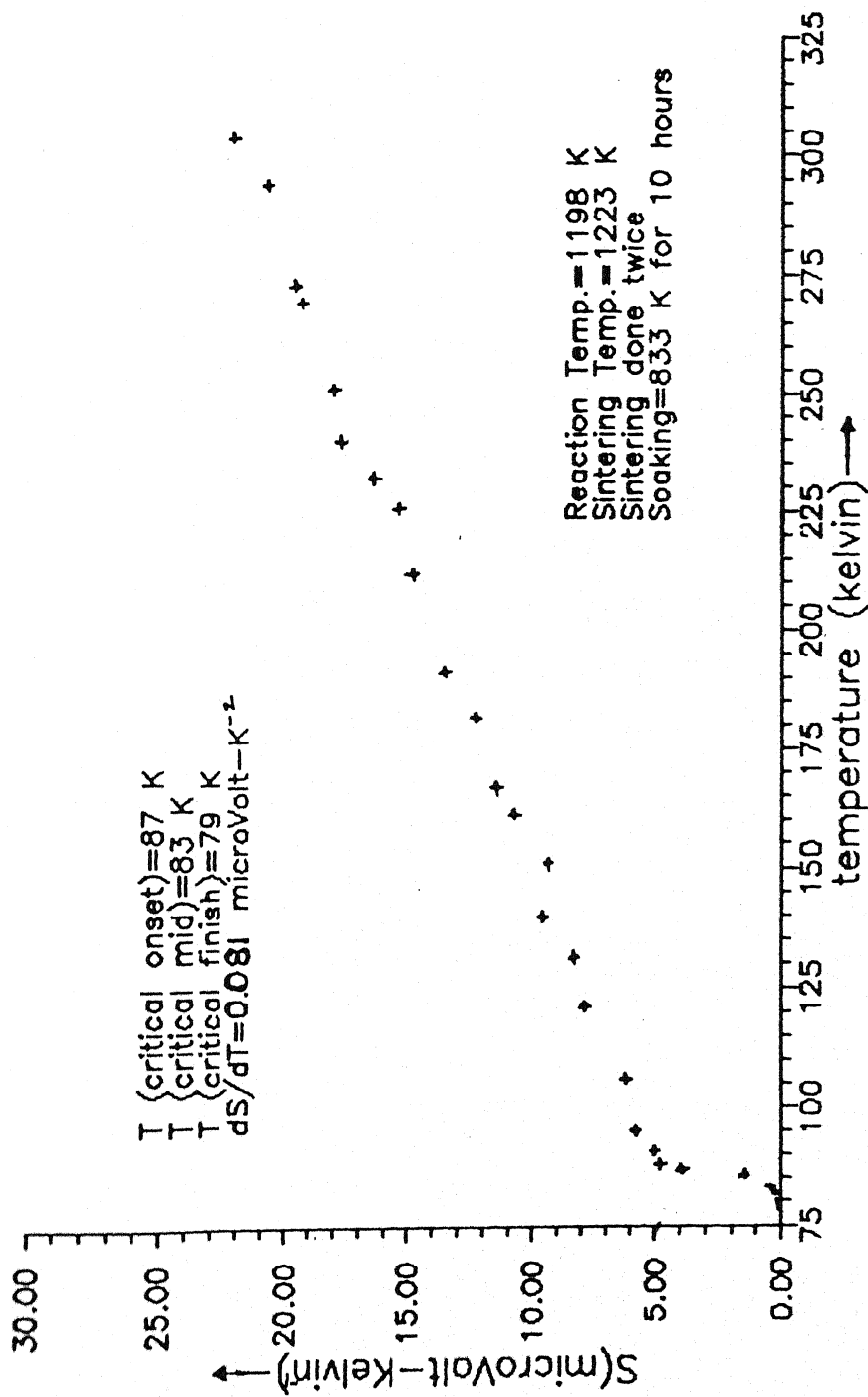
* All T_c values quoted from resistivity data.

T_c obtained from thermo electric power are slightly different.



System : Sm Ba_{1.5}CaCu₃O_{7-s} (Bi)

FIG. 3.14



System : $\text{SmBa}_{0.5}\text{Ca}_{0.5}\text{Cu}_3\text{O}_{7-\delta}$ (B_2)

FIG. 3.15

Figure 3.13 shows the same results (S vs. temperature) for A_2 samples which was prepared and processed at higher temperatures. The results are qualitatively similar to that for A_1 sample (Fig. 3.12). Both samples (A_1 and A_2) show positive thermo electric power suggesting that the charge carriers are holes rather than electrons.

3.4.2 THERMO ELECTRIC POWER OF Ca-DOPED Sm-Ba-Cu-O SAMPLES (B_1 and B_2)

Figure 3.14 shows the variation of thermo electric power as a function of temperature for B_1 sample ($\text{SmBa}_{1.5}\text{Ca}_{0.5}\text{Cu}_3\text{O}_{7-\delta}$) which was prepared and processed at lower temperatures. The thermo electric power remains positive over the entire temperature range which suggests that the charge carriers are holes. Further, the thermo electric power decreases linearly ($dS/dT = 0.090\mu\text{V K}^{-2}$) as the temperature decreases upto the critical temperature and drops suddenly to zero at T_c and remains zero in the superconducting state.

Figure 3.15 shows the same results (S Vs. T) for B_2 samples ($\text{SmBa}_{1.5}\text{Ca}_{0.5}\text{Cu}_3\text{O}_{7-\delta}$) which was treated at higher temperatures. The main features are similar to earlier results, that is S is always positive (holes are the carriers), has linear dependence on temperature at $T > T_c$ and becomes zero at $T \leq T_c$ and $dS/dT = 0.081\mu\text{V K}^{-2}$.

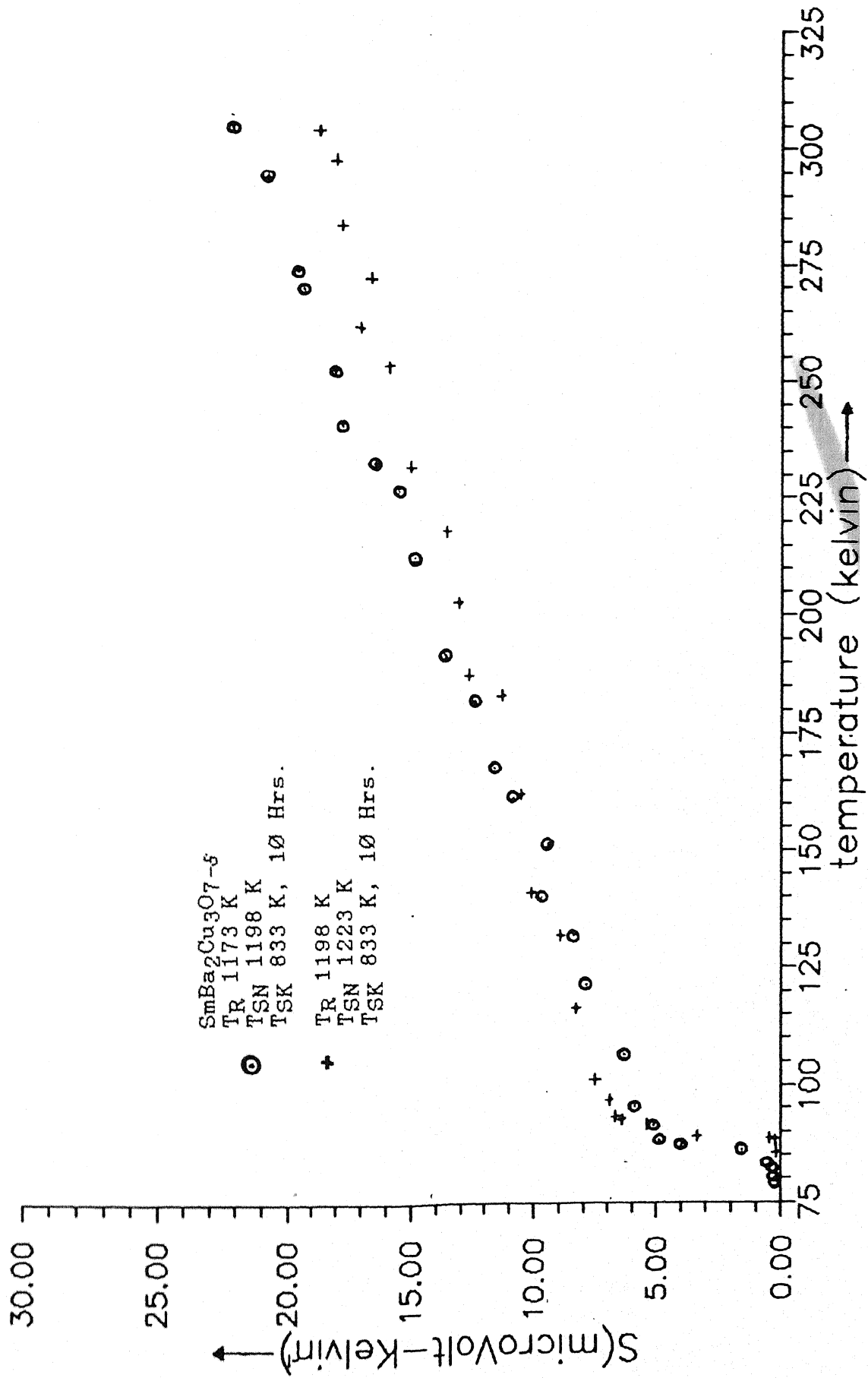
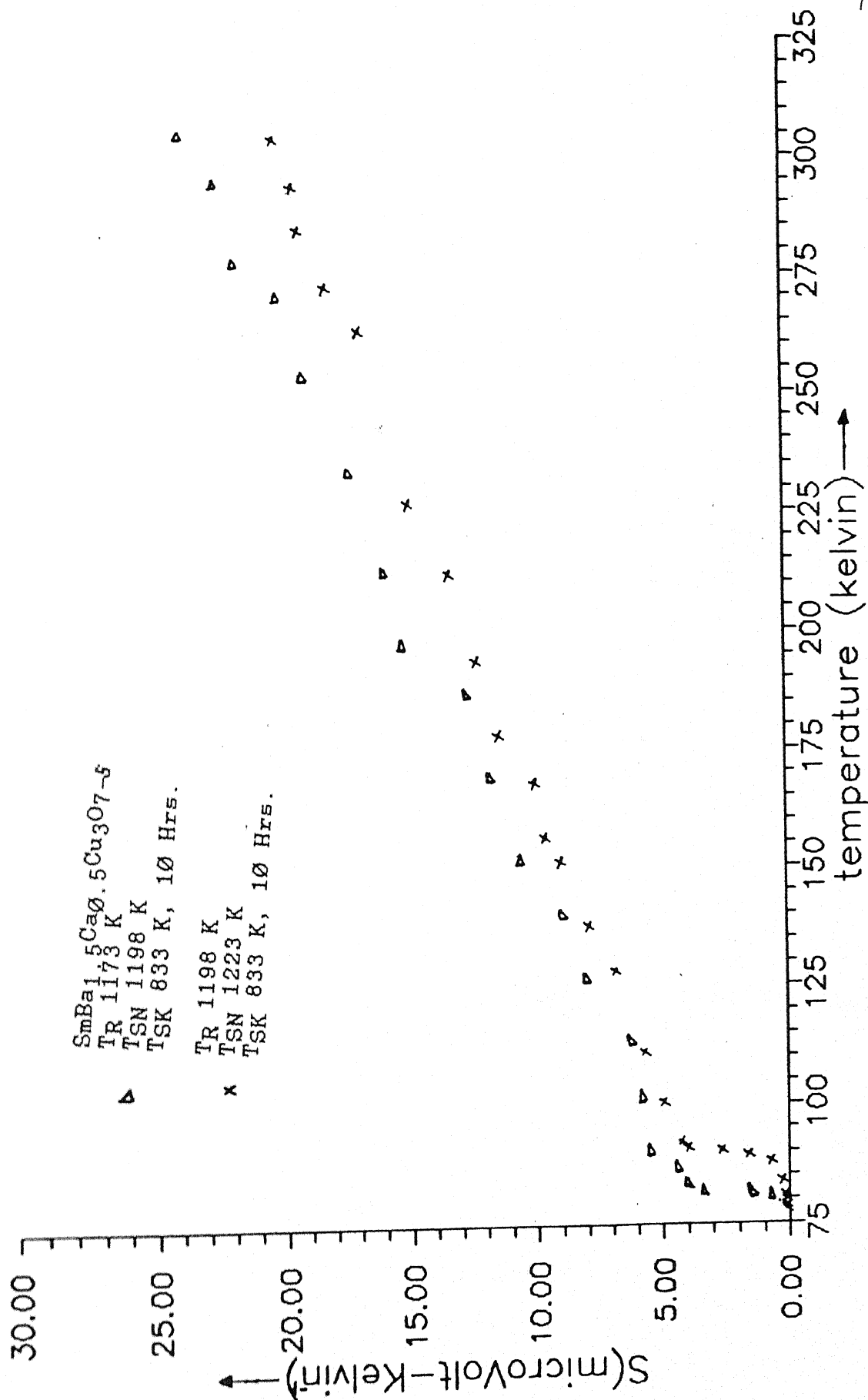


FIG. 3.16 (A₁-A₂)

3.4.3 THE EFFECT OF HEAT TREATMENT

The thermopower results of all the four samples, pure samples (A_1 and A_2) and two doped samples (B_1 and B_2) are compared in Table 3 along with those of $YBa_2Cu_3O_{7-\delta}$ and earlier studies on $SmBa_2Cu_3O_{7-\delta}$ (Ref: 22). It is found that the A_2 sample which was processed at higher temperatures than A_1 has a higher T_{cm} (89 K Vs. 85.5 K for A_1), lower thermoelectric power S_{RT} (18.6 Vs. 20 $\mu V K^{-1}$ for A_1) and more significantly lower width of transition ΔT (5K Vs. 11K for A_1).

These results, together with XRD and resistivity studies, clearly suggest that the sample A_2 prepared and processed at higher temperatures exhibits better superconducting properties. It should be pointed out that the width of the critical region $\Delta T = T_{co} - T_{cz}$ (O refers to onset and z completion (zero resistance) of transition) is a good representative of the quality of the superconducting material; narrower (small ΔT) the critical region better is the material, just as sharper is the melting transition purer is the salt. An interesting result in support of this is reported by Lee et.al.²² who found that $YBaCuO$ quenched in O_2 had a, $\Delta T_c = 13K$ while for O_2 -cooled $YBaCu_3O_{7-\delta}$ sample a $\Delta T_c = 3.3K$ only. It is now a well known that slow cooling in O_2 -atmosphere is necessary to obtain the excess-oxygen-containing ortho-phase which is superconducting. Good samples of Y-Ba-Cu-O have as low ΔT_c as (1-1.5K). Thus it is concluded that heat treatment has considerable effect on the quality of superconducting material. A_2 samples

FIG. 3.17 (B_1-B_2)

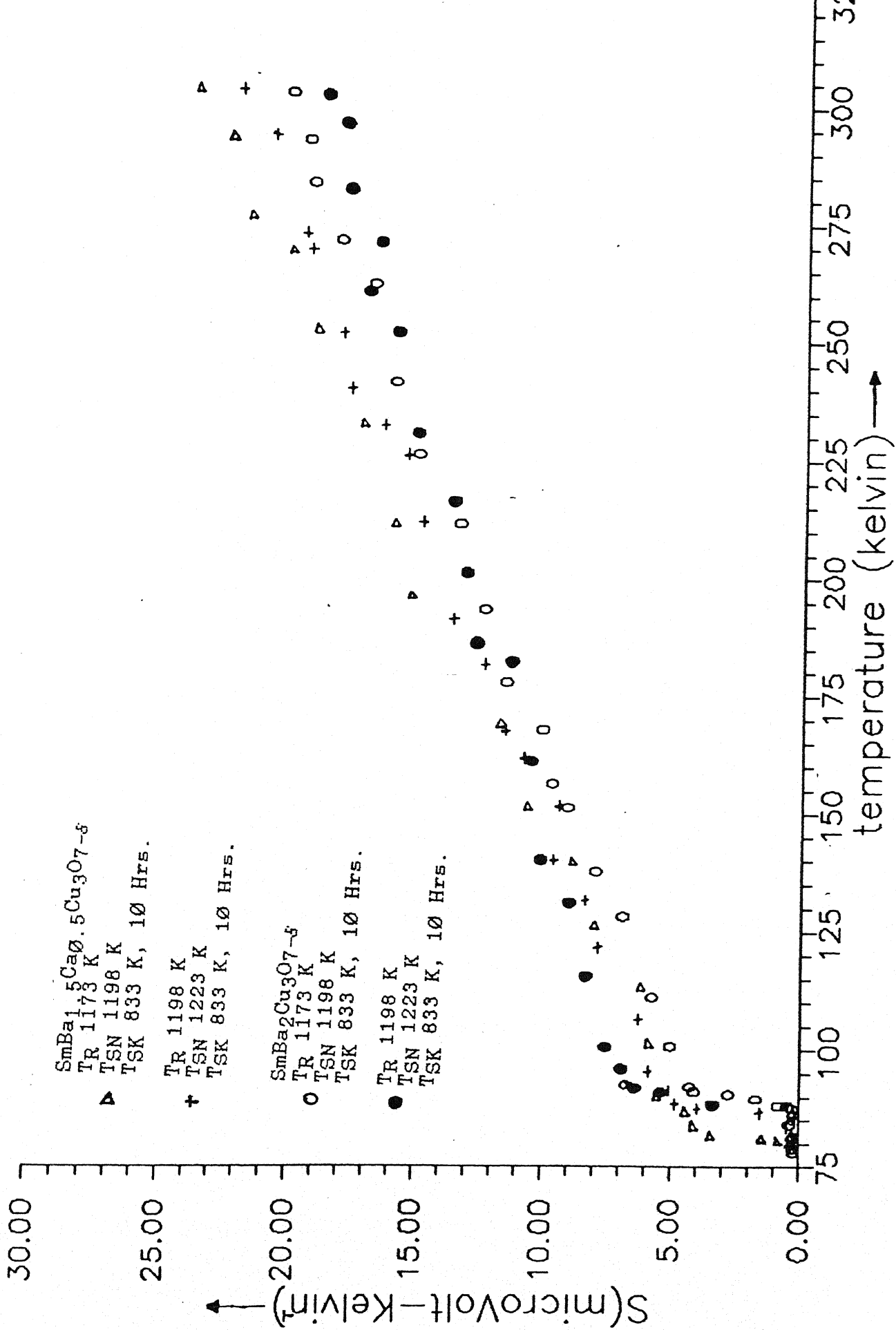


FIG. 118 ($A_1 = A_2 = B_1 = B_2$)

prepared and processed at $T_R = 1198\text{K}$ and $T_S = 1223\text{K}$ respectively exhibit better properties than A_1 samples ($T_R = 1173\text{K}$ and $T_S = 1198\text{K}$).

The effects of heat treatment on doped-samples B_1 and B_2 (Table 3) are similar to those observed for A_1 and A_2 samples. The B_2 sample treated at higher temperatures shows higher T_c , lower resistivity as lower thermo electric power. However, ΔT_c has unexpectedly increased.

3.4.4 EFFECT OF DOPING

As discussed earlier the effect of 25% doping by Ca^{2+} was to increase the resistivity. Likewise, the doped sample shows higher thermo electric power at room temperature, and a lower T_c value compared to undoped sample but heat treated identically.

3.4.5 COMBINED EFFECT OF DOPING AND HEAT TREATMENT ON THERMO ELECTRIC POWER

- (a) The pure SmBaCuO sample which was heat treated at higher temperature has lower S_{RT} and a bit higher T_c .
- (b) The pure SmBaCuO sample which was heat treated at lower temperatures than that of (a), has a higher S_{RT} and lower T_c than that of (a).
- (c) The Ca-doped SmBaCuO sample heat treated identically as (a) has still higher S_{RT} than (b) and lower T_c than (b).

TABLE 3

PROPERTIES OF PURE AND Ca-DOPED Sm-Ba-Cu-O HIGH T_c SUPERCONDUCTORS

Composition	T_c (K)		ΔT_c (K)		S ($\mu V K^{-1}$) at		$\frac{dS}{dT}$ ($\mu V K^{-2}$)
	T_{co}	T_{cm}	T_{cz}	R_T	T_{co}		
SmBa ₂ Cu ₃ O _{7-δ} (A ₁)	91.0	85.5	80.0	11.0	20	4	0.09
SmBa ₂ Cu ₃ O _{7-δ} (A ₂)	91.5	89.0	86.5	5.0	18.6	6	0.08
SmBa _{1.5} Ca _{0.5} Cu ₃ O _{7-δ} (B ₁)	82.5	80.0	78.0	4.5	23.7	5	0.09
SmBa _{1.5} Ca _{0.5} Cu ₃ O _{7-δ} (B ₂)	87.0	83.0	79.0	8.0	22	5	0.10
SmBa ₂ Cu ₃ O _{7-δ} ²²	85.0	73.0	61.0	22.0	22	-	-
YBa ₂ Cu ₃ O _{7-δ} ²² (cooled in O ₂)	95.5	94.0	92.2	3.3	-2.7	-	-
YBa ₂ Cu ₃ O _{7-δ} ²² (Quenched in O ₂)	80.3	71.8	67.3	13.0	18.0	-	-

- (d) The Ca-doped SmBaCuO sample which was heat treated identically as (b), has higher S_{RT} and lowest T_c of all.

3.5 CONCLUSION

Pure and Ca-doped Sm-Ba-Cu-O high - T_c superconductors were prepared under two differing conditions to examine the effect of preparational conditions and doping. All samples have been examined by XRD and their resistivity and thermoelectric power measured. The samples (both pure and Ca-doped) which were prepared and sintered at higher temperatures, 1198K and 1223K respectively, show a higher T_c smaller width of transition (ΔT_c), lower resistivity and thermoelectric power (Table 3 and Fig. 3.12 to Fig.3.18). The doping of $\text{SmBa}_2\text{Cu}_3\text{O}_{7-\delta}$ by 25% Ca in place of Ba has unfavourable effects. The resistivity & T_c are increased.

The thermoelectric power (S) and resistivity (ρ) measurements are found consistent as far as the values of T_c and the fact that S and ρ follow each other are concerned. Whenever the effect (of heat treatment or doping) was to increase (decrease the resistivity thermoelectric power also increased (decreased)). In all samples, the sign of thermoelectric power was always positive, both in normal state as well as superconducting state, suggesting that the holes are majority charge carriers. Similar results are reported for $\text{YBa}_2\text{Cu}_3\text{O}_{7-\delta}$.

Due to lack of theoretical models applicable to high T_c superconductors, a more detailed quantitative analysis of the transport studies has not been possible at this stage.

REFERENCES

1. H.K. Onnes, Communication, Phys. Lab. Univ., Leiden, 1206, 3 (1911).
2. Frohlich, H. 1950, Phys. Rev., 79, 845.
3. Bloch, F., 1928, Z. Phys. 52,555.
4. Casimir, H.B.G., 1953, Physica, 19, 764.
5. Onsager, L., 1944, Phys. Rev., 65, 117.
6. Ginzburg, V.L., 1952, USP. fiz. Nauk 48, 25 (German translation -- 1953, Fortschr. Phys. 1, 101).
7. Schafroth, M.R., 1955, Phys. Rev. 100, 463.
8. Schafroth, M.R., Butler, S.T., and Blatt, J.M., 1957, Helv. Phys. Acta, 30, 93.
9. Cooper, L.N., 1956, Phys. Rev. 104, 1189.
10. Bardeen, J., Cooper, L.N. and Schrieffer, J.R., 1957, Phys. Rev. 106, 162, Phys. Rev. 108, 1175.
11. Michel, C. and B. Raven, Rev. Chim Minar, 21, 407, 1984.
12. Bednorz, J.G. and K.A. Muller, 2 Phys. B, 64,189(1986).
13. Chu et al, Phys. Rev. Lett. 58 (1987), 405.
14. Wu et al, Phys. Rev. Lett. 58, 908(1987).
15. Maeda, H. Tanaka, Y. Fukutomi, M. and T. Asano; Japan Appl. Phys.27, L209 (1988).
16. Shen, Z.Z. and Hemen, A.M., Nature, 138, (1988).
17. Cava, R.J., Van Dover, R.B., B. Baltigg and Rietman, E.A., Phys. Rev. Lett., 54, 4, 408 (1987).
18. Meissner, W. and Ochsenfeld, R., 1933 Naturwissenschaften, 21, 787.

20. Logan, B.F., Rice and Wick, R.F., J. Appl. Phys. 42,7, 2975, (1975).
21. L. Cao et al., Superconductivity C, 139, (1989), 195-200.
22. S.C. Lee et.al., Phys. Rev. B, Vol. 37, No. 3, 37, 36, 1st Feb., 1988.
23. Charles.G. Kupper - An introduction to the theory of Superconductivity, Clarendon Press (Oxford), 1968.
24. Blackmore, J.S., Solid State Physics, Second edition, Cambridge University Press (1985).
25. Ehrenreich, H. and Turnbull, B., Solid State Physics, Vol. 42, Academic Press, (1988).